Journal of Neurocytology 1, 311–340 (1972)

Organelle formation from pinocytotic elements in neurites of cultured sympathetic ganglia

R. I. BIRKS,* MICHAEL C. MACKEY and P. R. WELDON

Physiology Department, McGill University, Montreal, Canada

Received 24 July 1972; revised 20 November 1972; accepted 29 November 1972

Summary

Chick embryo sympathetic ganglia were cultured for 36 h in the presence of NGF to establish a profuse neuritic outgrowth. The intracellular distributions of labelled and unlabelled organelles were determined with respect to time in these ganglia following reincubation for different periods with ferritin or thorium dioxide and fixation and preparation for electron microscopy. The distributions were in quantitative agreement with the hypothesis that multivesicular bodies are formed from pinocytotic vacuoles through intermediate structures we have named pre-multi-vesicular bodies. Under the conditions of our experiments the entire multi-vesicular body population turns over in about 2 h. We have also obtained evidence that these last structures are involved in the later formation of simple blind-ended tubules that we consider to be distinct from the endoplasmic reticulum. Marker was also found in a variety of dense-cored vesicles, many of which appear to form from pinocytotic vesicles. After prolonged incubation, large numbers of labelled organelles accumulated in the neuritic varicosities, which we have found to resemble closely the organelle accumulations at interrupted peripheral nerves. Thus the latter accumulations may arise in part from local formation as well as from somatofugal migration.

Introduction

Growth cones of living axons and other neuritic processes are well known to be sites of active pinocytosis (see for references, Pomerat *et al.*, 1967). It also appears from time-lapse cinematographic studies that, after formation, pinocytotic vacuoles and vesicles move within the axoplasm and breakdown to particles too small to be resolved by light microscopy (Pomerat *et al.*, 1967).

Because of the rapid outgrowth and high concentration of neurites noted in cultured chick embryo ganglia (Birks and Weldon, 1971), chick embryo sympathetic ganglia were selected to: 1. study the fate of ingested pinocytotic elements in growth cones; and 2. investigate to what extent they may contribute to the formation of subcellular organelles in the peripheral parts of the neurites.

* Medical Research Associate of the Medical Research Council of Canada.

Exposure of cultured ganglia to ferritin and thorium dioxide has permitted a quantitative approach to these two problems through determination of the time-varying distributions of various unlabelled and labelled organelles. The results of this study suggest a local formation of a variety of intracellular organelles from primary pinocytotic vesicles and vacuoles. Time-varying distributions of unlabelled and labelled vacuoles, multi-vesicular bodies, and structures intermediate in form between these two, provide quantitative support for the hypothesis that multi-vesicular bodies are formed from pinocytotic vesicles via intermediate structures we have named pre-multi-vesicular bodies. The multi-vesicular bodies in turn appear to be involved in the formation of tubular elements in the neurites. Our results also provide evidence that a variety of dense-cored vesicles are formed locally in the neurites. These findings suggest that the accumulation of organelles in compressed axons may result partly from local formation of the organelles, not entirely from somatofugal flow.

Methods

Culture procedure

Lumbar sympathetic chains from 12-day chick embryos were explanted onto collagen-coated coverslips, which had been covered with a carbon film (Robbins and Gonatas, 1964) prior to application of the collagen. The explants were overlaid with strips of dialysis membrane (Rose *et al.*, 1958), and a glass ring lightly coated with vacuum grease (Dow Corning Corp.) was pressed down on each coverslip forming a well. The well was then filled with tissue culture medium and the assembly was sealed with a second coverslip. The culture medium consisted, in parts ml^{-1} of: 7 parts synthetic medium 1066, 2 parts fetal calf serum, and 1 part 50% chick embryo extract. Glucose was added to a final concentration of 500 mg% and penicillin (100 units ml^{-1}) and streptomycin (100 μg ml^{-1}) were also present. Mouse submaxillary gland extract was added as a source of nerve growth factor (Birks and Weldon, 1971). Cultures were incubated for 36 h at 37°C in a humidified incubator, in a 95% O_2, 5% CO_2 atmosphere.

Preparation of ferritin and thorium dioxide

Horse spleen ferritin (10% solution, 2 × recrystallized, cadmium free; Nutritional Biochemicals, Cleveland, Ohio) was centrifuged for 2 h at 100000 *g*, washed once in distilled water, and redissolved in culture medium at a concentration of 10%. Thorium dioxide (25% colloidal suspension, Fellows Testagar, Anaheim, California) was treated in a similar manner and resuspended in culture medium at a concentration of 7%.

Experimental procedure

Preliminary experiments on uptake of ferritin into neurites of cultured sensory neurones (Birks and Weldon, 1971) showed that a long exposure of 6 h to 20% ferritin caused neuritic retraction and considerable cell necrosis. For the present experiments the concentration of ferritin was reduced to 10% and the maximum exposure time was reduced to 2 h. Under these conditions little damage to the tissue was seen.

The dialysis strips were removed from cultures that had been allowed to grow for 36 h. Each ganglion was then washed briefly in balanced salt solution and reincubated with warm (37°C) culture medium containing 10% ferritin or 7% thorium dioxide. In the ferritin experiments, the ganglia were exposed to the marker for 10, 30, 80 and 120 min, or for 120 min followed by a 120 min chase period before fixation. In the experiments with thorium, chase periods of 2 and 16 h were given.

Cultures were prepared for electron microscopy by fixation for 1 h in 3.5% glutaraldehyde in

0.1 M phosphate buffer, pH 7.2 at 5°C. The cultures were postfixed in 1% OsO_4 for 1 h at 5°C and stained overnight in 0.5% aqueous buffered uranyl acetate. Following dehydration in graded ethanol, the cultures were embedded in Epon 812 by inverting a gelatin capsule filled with the resin over the explant. After polymerization at 65°C for 24 h, the capsules containing the explant and underlying collagen substrate and carbon film were pulled away from the coverslip and appropriate areas for sectioning were located on the block face using a dissecting microscope. Thin sections for electron microscopy were cut on a Huxley microtome, mounted on carbon-coated grids and stained with lead citrate. Usually this combined block and section staining procedure gave high contrast. Occasionally sections were further stained with a saturated aqueous solution of uranyl acetate.

Counting of ferritin-labelled organelles

In the series of experiments that forms the bulk of this study the distribution of ferritin in the neurites after periods of 10, 30, 80 and 120 min exposure to marker, was determined quantitatively. The data for each incubation period were derived from three to four different ganglia. The total number of labelled and unlabelled organelles in three classes of organelles were counted to totals of about 1000 in each class. The sections of tissue from which the counts were derived were then photographed and estimates made of the area of the neurites within them. This latter procedure has one major source of error: because of the low contrast of the Siemens microscope at low magnification it was difficult to recognize the tissue areas which contained fibroblasts with accuracy. Therefore, the area measurements are accurate to not better than $\pm$ 20%.

Results

MORPHOLOGY OF THE NEURITIC OUTGROWTH

The main morphological elements of neuritic outgrowth in living cultured chick dorsal root ganglia and sympathetic ganglia have been described at the light microscope level of resolution by Pomerat *et al.* (1967). As the neuritic outgrowth is followed from its origin in the explanted ganglion, periodic dilatations or varicosities are found. More distally small beaded regions containing large vacuoles occur. The neurites terminate in a growth cone, which usually consists of a dilated varicosity merging with a flange of undulating membrane of variable form, frequently associated with spike-like projections, called microspikes. It will be convenient to describe the fine structure of the outgrowth with reference to these structural elements.

Neurites

The diameter of the neurites varied usually from 0.2–1.0 μm. Figs. 1–4 illustrate the varieties of structural organization found in them. They contained a variable population of microtubules and neurofilaments, embedded in a filamentous meshwork of fine (50–60 Å) short interwoven filaments, similar to that described by Yamada *et al.* (1971) for axons in cultured chick dorsal root ganglia. Smooth-surfaced tubular structures, with periodic dilatations and branchings were distributed along the course of the neurites. None of these elements appeared to occupy preferentially a distinct region of the cytoplasm. The neuritic complement of other organelles was very variable and generally sparse, it included mitochondria, electron-lucent, dense-cored, and coated vesicles; and a variety of multi-vesicular and

multi-cored bodies, with shapes varying from spherical to elongated tubular forms more than 1 μm in length. Identifiable ribosomal particles were not seen in the neurites, although they have been reported in axons of embryonic dorsal root ganglia of the chick (Yamada *et al.*, 1971) and of the rabbit (Tennyson, 1970).

Varicosities

Dilatations of the neurites not associated with growth cones were a prominent feature of the neuritic outgrowth. They varied in diameter from 1.5–3.5 μm, and in length from 3–7 μm. It was possible to distinguish two general types of varicosity. In one (Fig. 5) the cytoplasm was occupied almost exclusively by a branched tubular system with periodic cisternal dilatations, the whole being embedded in a filamentous meshwork similar to that observed in the neurites. The second type (Fig. 6) was characterized by the presence of large numbers of different types of organelles, with a scanty distribution of branched tubules, but with many short blind-ended tubular elements. The types of organelle characteristic of the second type of varicosity consisted of mitochondria, multi-vesicular bodies of all forms, smooth-surfaced vesicles and vacuoles, and myelin bodies. They also contained infrequent coated and dense-cored vesicles, but the latter were difficult to distinguish from cross-sectional views through tubular multi-vesicular bodies. The division into two types was not always completely sharp, in many of the former type, occasional mitochondria and vesicles were found, and in the latter type, discrete areas of the varicosity contained collections of branched tubules.

The two types of membrane-bounded tubules described above appear to be morphologically distinct. The branched tubules interspersed with dilated cisternae have a very irregular outline and a labyrinthine dispersion, and their appearance coincides with what is usually described as smooth-surfaced endoplasmic reticulum. On the other hand the tubular elements of Figs. 6 and 9 can be seen to be characteristically blind-ended. Their course is usually straight or gently curving, and their diameters are quite regular, varying usually from 600–800 Å, about the same as for the tubular multi-vesicular bodies. Thus on purely morphological grounds these two types of membrane-bounded tubules do not appear to form part of the same system. This is supported by their different modes of tracer uptake described below. So we shall distinguish between them by calling the long, narrow and

---

Figs. 1–4 provide longitudinal views through neurites showing the variations in organelle density and organelle types.

Figs. 1 and 2 show a predominant microtubular population and a predominant neurofilament population respectively in two neurites. A meshwork of 50–60 Å diameter filaments is prominent in Fig. 1 (double arrows).

Figs. 3 and 4 show more mixed populations of organelles in two neurites. Note the varieties of forms of multi-vesicular bodies in Figs. 2, 3 and 4; the two facing cup-shaped vesicles enclosing a noticeably electron-lucent space in Fig. 3 (arrow); and the two coated vesicles in Fig. 4 (single arrows) one of which contains a dense core. Double arrows show areas where the filamentous meshwork is prominent. Black bars in these and all following figures represent 0.5 μm, except where stated specifically in the legends. Only one magnification bar is shown in Figs. 1–4, 8–9 and 13–21, where each figure is at the same magnification.

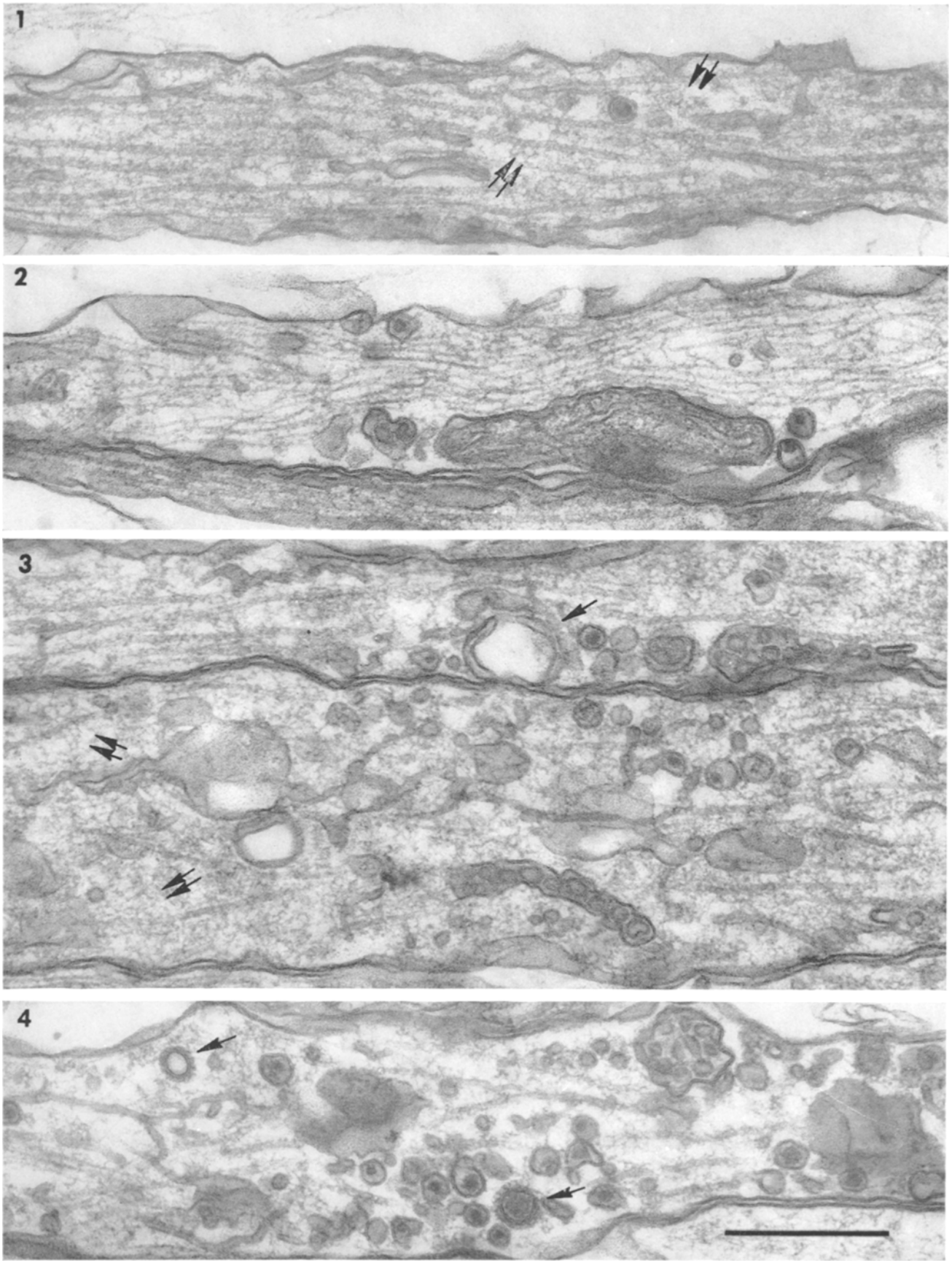
1
2
3
4


5

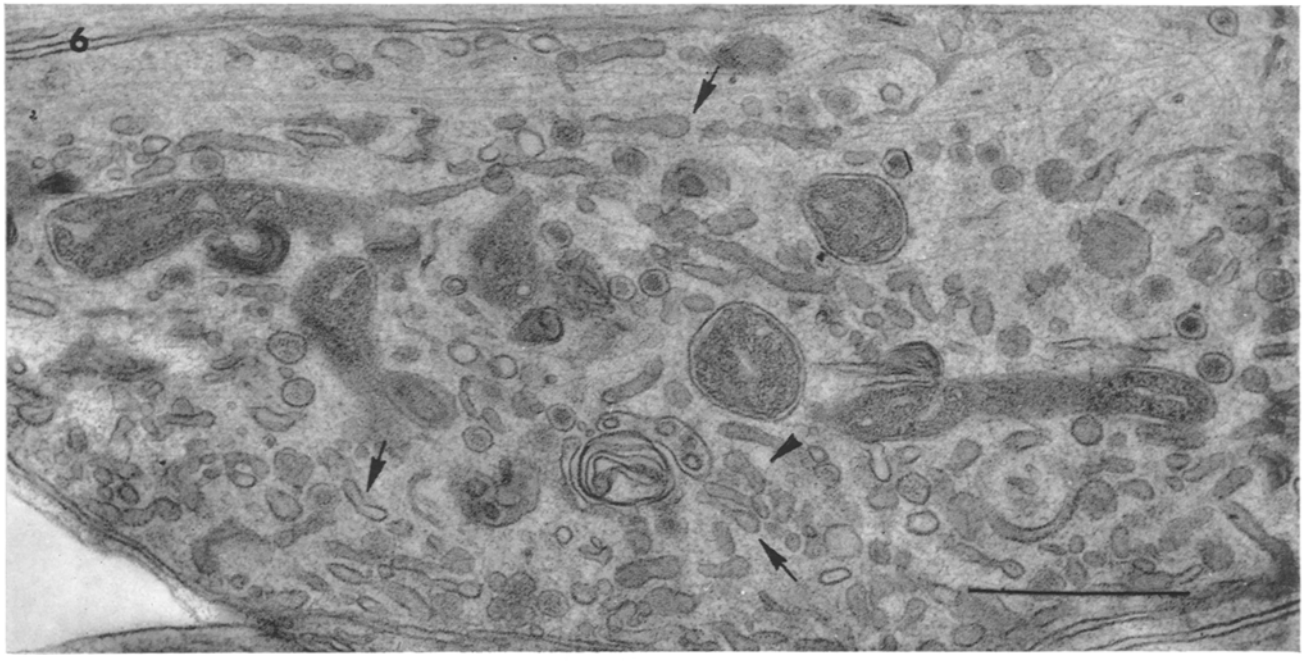
6

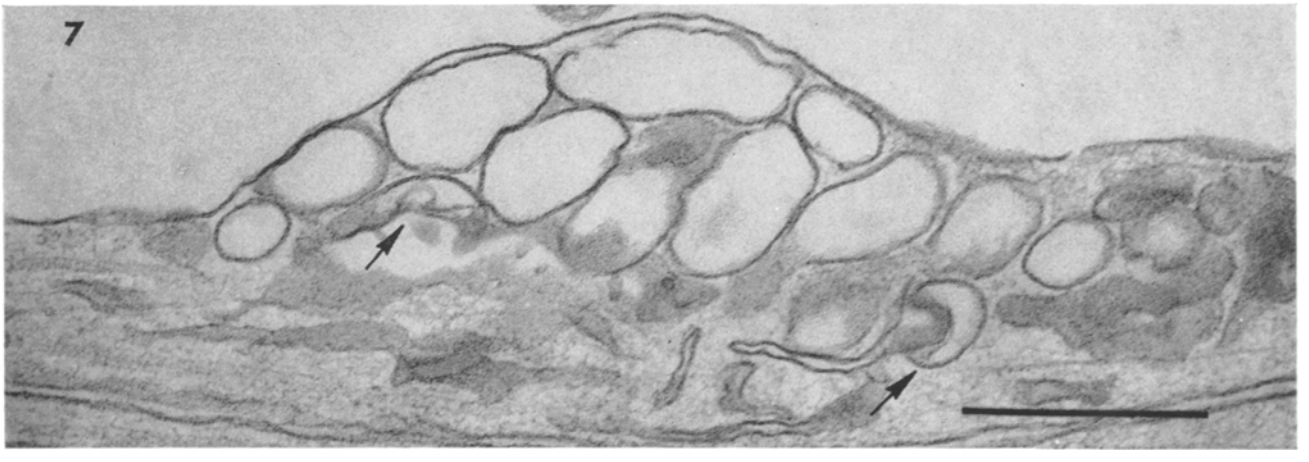
7

irregular ones 'axonal endoplasmic reticulum' and by calling the shorter, fatter, and smoother ones 'blind-ended tubules'.

It is worth noting here the very close similarity between the subcellular organization of the second type of varicosity and the terminal dilatations of regenerating peripheral nerve in mature animals (for general references see Martinez and Friede, 1970, and particularly Pellegrino de Iraldi and de Robertis, 1968; Zelená *et al.*, 1968; Kapeller and Mayor, 1969). Similarities between the terminal dilatations associated with growth cones in other embryonic and neonatal nervous tissue and regenerating nerve have been emphasized recently by Tennyson (1970).

Beaded dilatations

Small dilated regions of the neurite were frequently observed (Fig. 7). They usually consisted of a lateral expansion of the neurite with a diameter of 0.5–1.0 μm and a length of 0.7–2.0 μm, and they differed from the varicosities both in overall size and in organelle content. They were packed with vesicles and vacuoles from 0.05–0.5 μm in diameter, and with crescent-shaped profiles, which appeared to be sections though saucer- or cup-shaped vacuoles, somewhat similar to those observed in the adrenal medulla (Holtzman and Dominitz, 1968). Frequently these structures were associated with a void, electron lucent region or with one or more spherical vesicles. A more complete description of these elements is given below in considering the uptake of ferritin into the neurites.

Growth cones

Unequivocal identification of these elements of the neurites was not always possible, but growth cones could be identified in favourable sections by the presence of small filopodia (Tennyson, 1970), or microspikes (Yamada *et al.*, 1971) or by their irregular shape and pitted surface (Figs. 8 and 9). The size of the growth cones was slightly larger than that of the varicosities, being from 2–4 μm in diameter and up to 8 μm in length. The long microspike projections of growth cones found in other tissues were not a characteristic feature of these sympathetic neuritic terminations. On the other hand, like the growth cones of embryonic dorsal root ganglion cells (Yamada *et al.*, 1971) and of neonatal cerebral tissue (Kawana *et al.*, 1971), the most prominent intracellular feature was a dense meshwork of

---

Fig. 5 shows one type of non-terminal varicosity with an extensive matrix of randomly dispersed filaments, and containing scattered microtubules, prominent smooth-surfaced, branched interconnected tubules and cisternae, typical of endoplasmic reticulum.

Fig. 6 shows a second type of non-terminal varicosity containing a mixed population of organelles embedded in a filamentous matrix including mitochondria, multi-vesicular bodies, myelin bodies, dense-cored and simple vesicles, microtubules, neurofilaments. These organelles lie amongst a profusion of short, smooth-surfaced tubules, many of which appear blind-ended (arrows).

Fig. 7 shows a 'beaded region' of a neurite with typical accumulation of smooth-surfaced vacuoles and vesicles. Note the two cup-shaped vacuoles (arrows).

fine filaments. They also contained variable amounts of endoplasmic reticulum and blind-ended tubules (cf. Figs. 8 and 9). These tubular systems occur in considerable profusion in the growth cones of the tissues noted above and they have been described by Tennyson (1970), Yamada *et al.* (1971) and by Kawana *et al.* (1971) as endoplasmic reticulum, with the suggestion of a somal origin. Vesicles and vacuoles of a wide size range were prominent, located either near the plasmalemma or, equally characteristically, grouped in the centre of the cytoplasm. Dense-cored vesicles and tubular or spherical multi-vesicular bodies were also prominent but with no characteristic location. Usually not more than a single mitochondrion was present, and the overall organelle population was usually less than was found in the varicosities.

INTRACELLULAR DISTRIBUTION OF FERRITIN WITH DIFFERENT PERIODS OF INCUBATION

10, 30, 80 and 120 min incubations

The intracellular location of ferritin in the various parts of the neurites was examined after exposing ganglia to the marker for periods of 10, 30, 80 and 120 min. Regardless of the period of incubation, ferritin was never found free in the cytoplasm or in mitochondria. However, it was found in a wide variety of vesicles and vacuoles, from small vesicles 500 Å in diameter to large vacuoles over 0.5 μm in diameter, particularly with the shorter incubation times. Clusters of these elements were found in growth cones (Fig. 10) and characteristically in beaded regions (Figs. 11 and 12). In addition, cup-shaped vacuoles were prominent amongst the labelled organelles (Figs. 13–19). Sometimes these vacuoles appeared as ring-shaped profiles, which probably represent cross-sections through the rim of a cup (Fig. 18). The concentration of ferritin in the cup-shaped vacuoles was noticeably higher than in nearby spherical vesicles (cf. Fig. 11 with Figs. 13, 14 and 15). This could indicate that cup-shaped vacuoles form by loss of fluid and collapse of spherical vacuoles. In addition, it will be shown below that cup-shaped vacuoles appear to form multi-vesicular bodies; so we will refer to them as pre-multi-vesicular bodies. Some of these cup-shaped vacuoles contained vesicles, with or without dense-cores, or contained free dense granules. These

---

Fig. 8 shows a growth cone, which displays an irregular membrane profile and vacuolar inclusions (arrows). Note the extensive meshwork of fine filaments and scattered microtubules, the absence of mitochondria, and the prominent population of dense-cored vesicles. Endoplasmic reticulum predominates, with some blind-ended tubules visible.

Fig. 9 shows a growth cone which exhibits a pinocytotic invagination (double arrows) and an exceptionally dense population of organelles. Note particularly the dense-cored vesicles, and tubular multi-vesicular bodies, some of which contain dense cores rather than clearly defined interior vesicles (arrows). Here the blind-ended tubules predominate, and there is little endoplasmic reticulum. The similarity in diameter of dense-cored vesicles and tubular multi-vesicular bodies makes it difficult to distinguish between cross-sections through the latter structures and the dense-cored vesicles.

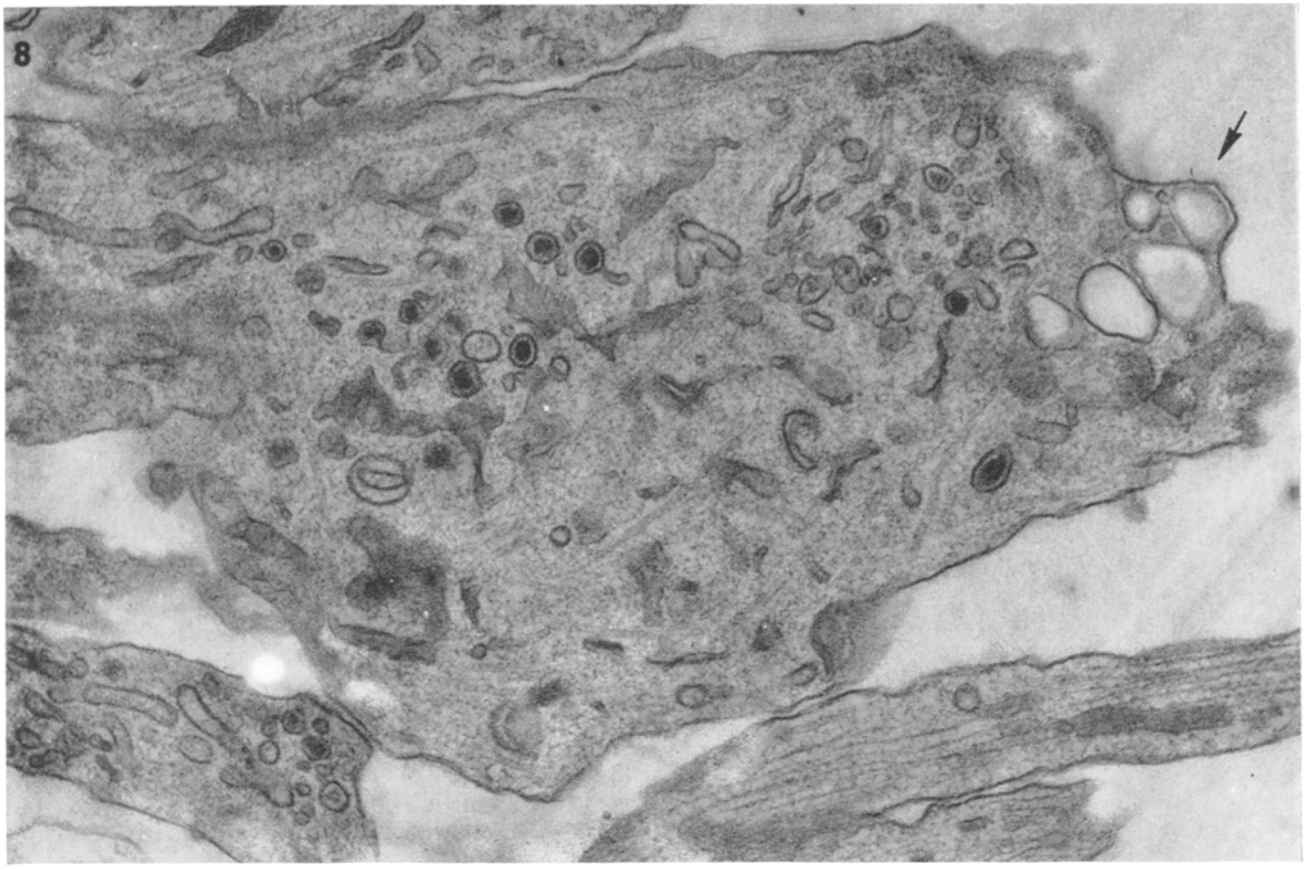
8

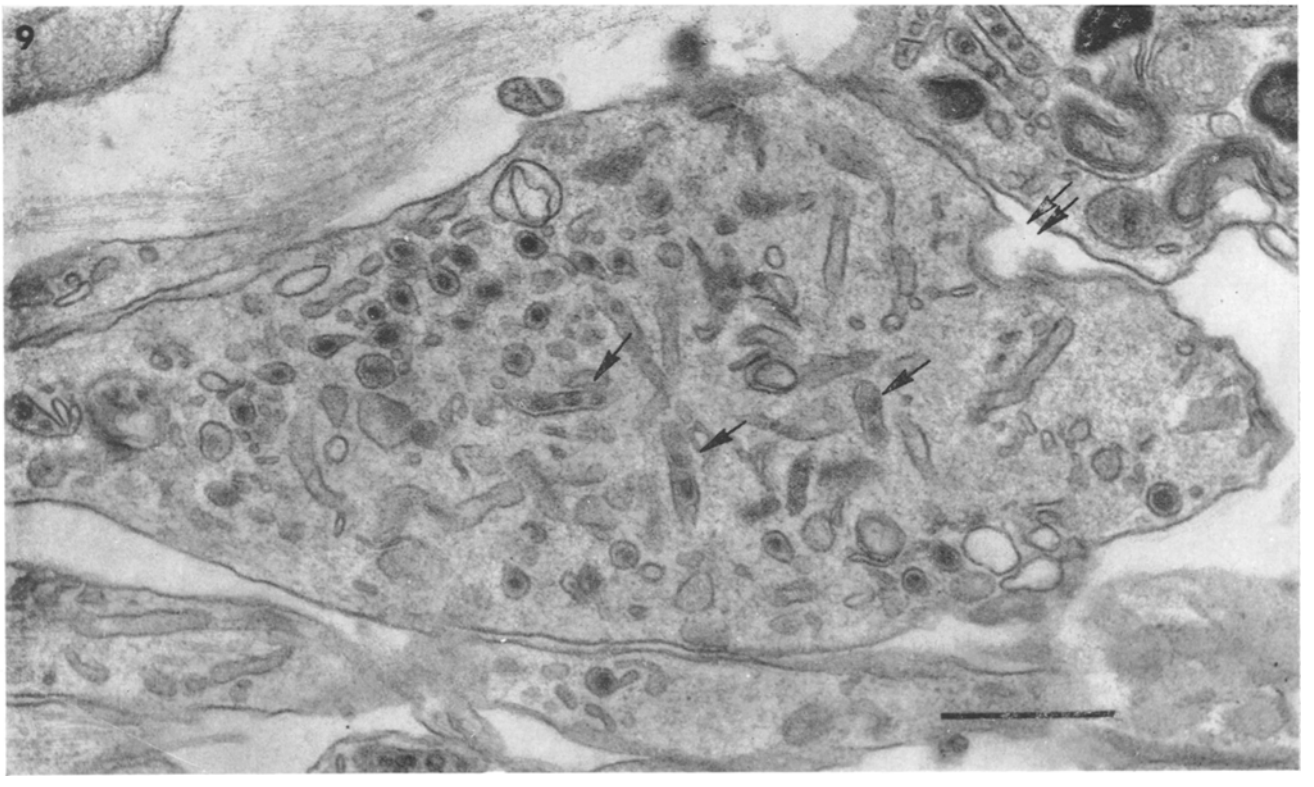
9

contents were sometimes distributed throughout the cup (Fig. 19); but more often they were located in the expanded rim of the cup (Figs. 16 and 17).

At the longer incubation times labelled organelles were present throughout the neurites and there were large accumulations in the nonterminal varicosities (Fig. 22). At these later times ferritin was especially concentrated in multi-vesicular bodies. These bodies were not always spherical; often they were elongated into tubules with an irregular diameter of 700–1300 Å, extending from 0.5–1.5 μm in length, and containing as many as 20 internal vesicles (Figs. 27 and 30). Frequently the internal vesicles contained a dense matrix, and sometimes they appeared simply as dense circular profiles with no limiting membrane. Often the more elongated forms tended to have a very regular diameter of about 700 Å, and frequently under these circumstances the number of internal elements was small (Fig. 31). By contrast, highly irregular forms of these tubular multi-vesicular bodies were also present, and some of them suggested a relationship between the cup-shaped vesicles and the tubular multi-vesicular bodies. Fig. 26 shows a tubular multi-vesicular body containing ferritin and internal vesicles, which displays a distinctly cup-shaped terminal portion (see also Fig. 28). In Fig. 25 the tubular multi-vesicular body is continuous with a ring-shaped terminal portion, presumably a cross-sectional view through the cup-shaped vacuole of the pre-multi-vesicular body.

Blind-ended tubules, devoid of interior vesicles, and with a regular diameter also occasionally contained ferritin, but we were unable to identify ferritin in the endoplasmic reticulum, however, see below the experiments with thorium dioxide. Marker was also seen in coated vesicles (Figs. 46 and 47) and in dense-cored vesicles (Figs. 40–44). After a 2 h incubation, 50% of the former organelles contained marker but these labelled vesicles represented only 3–4% of the total number of labelled organelles. At this same time, only 4% of the dense-cored vesicles were labelled and these comprised only 2% of the total number of labelled organelles. By far the greatest numbers of labelled organelles, however, were the vacuoles, cup-shaped vacuoles and multi-vesicular bodies, and even a preliminary survey of the tissue at different periods of incubation indicated a progressive shift of the label from vacuoles to multi-vesicular bodies. This suggested that vacuoles form by macropinocytosis, collapse into cup-shaped vacuoles, and acquire internal vesicles to become multi-vesicular bodies.

To evaluate this possibility we counted all vacuoles larger than 0.15 μm in diameter, all

---

Fig. 10 shows a growth cone from a 10 min ferritin experiment. Note the presence of ferritin in large smooth-surfaced vacuoles, which occupy the central region of the growth cone, and the high concentration of marker in the two cup-shaped vacuoles (single arrows). The two double arrows indicate surface invaginations.

Fig. 11 shows a beaded region of a neurite from a 10 min ferritin experiment. Note the presence of ferritin in a wide size range of smooth-surfaced vacuoles from 0.75 μm diameter to vesicles of about 0.05 μm diameter (arrow). In some of these only one or two ferritin particles are present.

Fig. 12 shows a beaded region from a 10 min ferritin experiment. Ferritin is most concentrated in the cup-shaped vacuole (arrow).

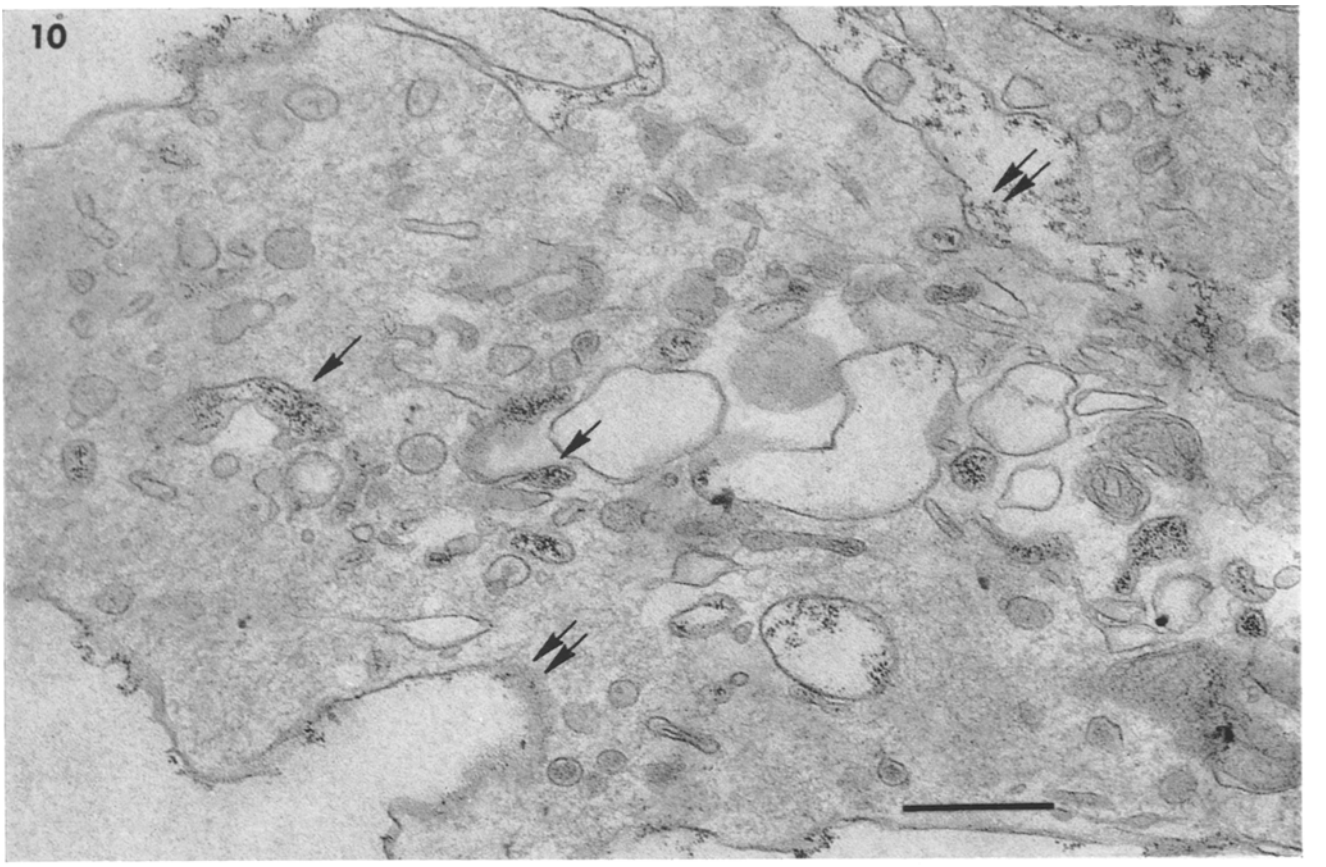
10

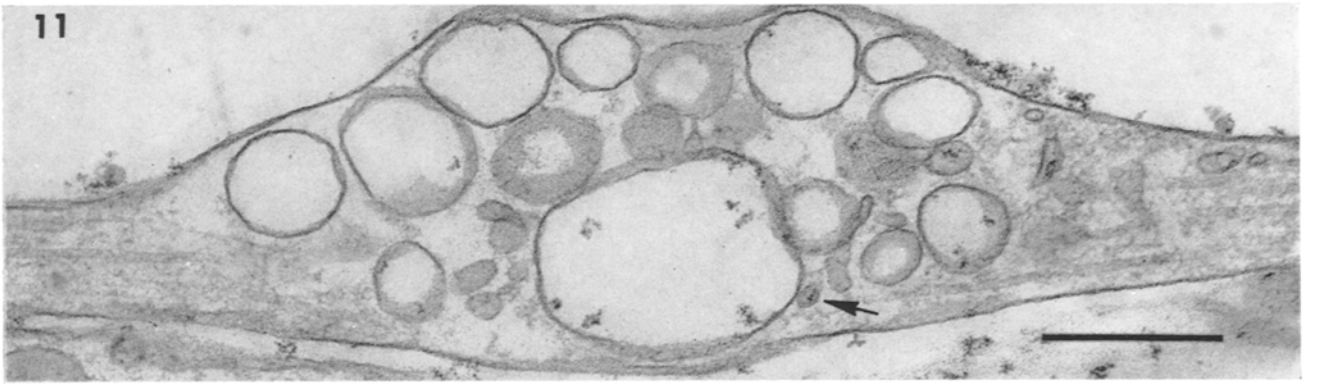
11


12


13


14

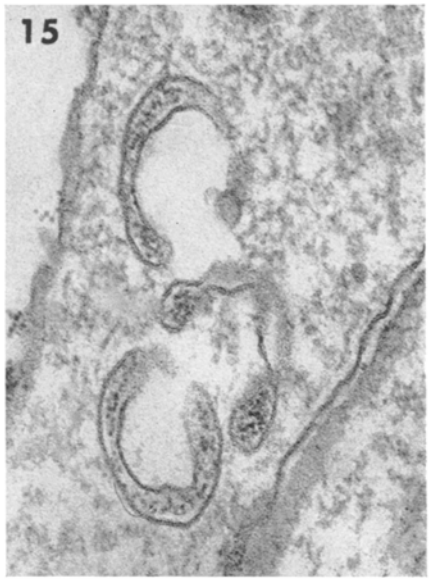
15


16


17


18

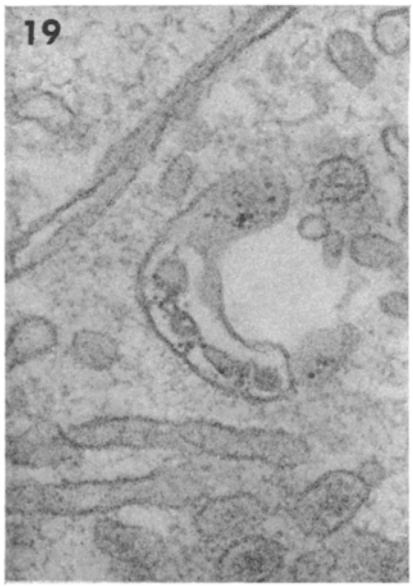
19

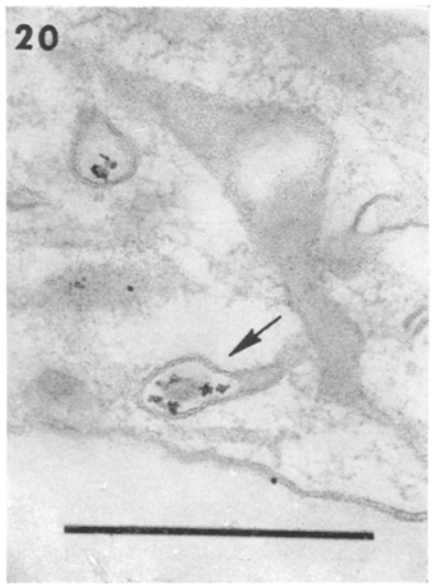
20

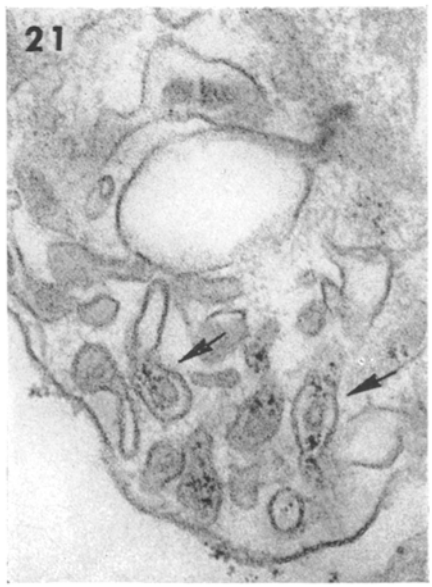
21

pre-multi-vesicular bodies, and all multi-vesicular bodies, both with and without ferritin in all neurites over one grid square (100 μm × 100 μm) in each of three or four sections from three or four ganglia, until a total of about 1000 was accumulated. In addition, we determined the area of tissue containing this number of organelles. The results of this procedure are given in Table 1. To serve as a reference, similar counts were made of two ganglia that had not been exposed to ferritin, or to the change of medium, after the 36 h growth period. These ganglia were chosen to illustrate the wide range of organelle densities that occurred in unincubated tissue: 36 as compared with 4 organelles per 100 μm^2 of tissue. This variation may represent differences in the rate of uptake of extracellular material, or in the rate of growth or retraction.

Table 1 illustrates that all tissues incubated in ferritin had high organelle densities. As incubation was lengthened, this organelle density did not increase further, but the distribution of label within the organelles changed. Table 2 shows the fractions of labelled and unlabelled organelles counted in each grid square at each time period, and this information is displayed in Fig. 34. It can be seen in Fig. 34a that the population of unlabelled vacuoles declined exponentially with time, whereas the population of labelled vacuoles increased during the first 30 min, such that about 25% of the total population was labelled; thereafter this population too declined in exponential fashion. It seems reasonable to suppose that upon immersion in ferritin there was no further production of unlabelled vacuoles, and thus the decline in this population with time represents the normal turnover time, whereas the more complex relationship between the labelled population and time reflects a combination of rapid early formation and later turnover. The unlabelled pre-multi-vesicular body population remained relatively constant for the first 30 min and thereafter declined exponentially (Fig. 34b). The labelled population increased rapidly over the first 80 min, at which time it comprised 90% of the total pre-multi-vesicular body population, and it then

---

Figs. 13 to 19 illustrate the varieties of pre-multi-vesicular bodies found throughout the neurites.

Figs. 13, 14 and 15 are from 30 min ferritin experiments and they show cup-shaped vacuoles containing large numbers of ferritin particles. In one case (Fig. 13) a cluster of small vesicles lies along the inner margin of the cup, and only one of these contains ferritin (arrow). In Fig. 14 the cup-shaped vacuole is associated with a single large spherical vesicle which contains no marker and in Fig. 15 the inner margins of three cup-shaped vacuoles are occupied by distinctly electron lucent areas.

Fig. 16 from a 120 min thorium experiment, and **Figs. 17, 18 and 19** from 30 min ferritin experiments demonstrate the presence of the markers in cup-shaped vacuoles which also contain interior vesicles or dense cores. In Figs. 16 and 17 the interior elements are located in the expanded rims of the cups, and in Fig. 19 they are distributed throughout. Fig. 18 shows a cross-sectional view through the rims of two cup-shaped vacuoles containing interior vesicles. In Figs. 14 and 16 note the presence of marker in simple tubules (double arrows).

Fig. 20 from a 120 min thorium experiment and **Fig. 21** from a 30 min ferritin experiment show structures somewhat related to those of Figs. 16 to 19 (arrows). They have the appearance (arrows) of short dense-cored tubules or dense-cored vesicles with tails. Similar structures have been noted by Teichberg (Holtzman, 1971) in this tissue and interpreted differently.

Table 1. Counts giving distribution of ferritin labelled and unlabelled organelles as a function of time of incubation with ferritin

Incubation time (min)	Grid number	Vacuoles			Pre-multi-vesicular bodies			Multi-vesicular bodies			Total organelles counted	Organelle density (number per 100 μm^2)	Pre-MVB plus MVB density (number per 100 μm^2)
		Unlabelled	Labelled	Total	Unlabelled	Labelled	Total	Unlabelled	Labelled	Total			
0	1	323		323	48		48	58		58	429	36	9.0
	2	82		82	22		22	40		40	144	4	1.7
10	3	133	40	173	38	24	62	25	5	30	265	31	11.0
	4	212	42	254	38	25	63	36	7	43	360	22	6.5
	5	128	25	153	40	23	63	47	4	51	267	24	10.0
30	6	158	58	216	56	67	123	45	25	70	409	20	9.0
	7	184	58	242	74	101	175	38	47	85	502	28	14.0
	8	218	69	287	27	66	93	61	47	108	488	29	12.0
80	9	106	27	133	26	117	143	9	32	41	317	15	8.5
	10	98	24	122	20	109	129	14	42	56	307	11	7.0
	11	96	24	120	7	74	81	28	83	111	312	13	8.0
	12	69	21	90	11	82	93	15	63	78	261	15	10.0
120	13	24	14	38	5	40	45	2	68	70	153	15	11.5
	14	44	7	51	14	94	108	8	132	140	299	12	10.0
	15	55	19	74	18	90	108	12	162	174	356	9	7.0

Table 2. Fractional distribution of labelled and unlabelled organelles as a function of incubation time

Incubation time (min)	Grid number	Vacuoles			Pre-multi-vesicular bodies			Multi-vesicular bodies		
		Unlabelled	Labelled	Total	Unlabelled	Labelled	Total	Unlabelled	Labelled	Total
0	1	0.75		0.75	0.11		0.11	0.14		0.14
	2	0.57		0.57	0.15		0.15	0.28		0.28
	Mean	0.66		0.66	0.13		0.13	0.21		0.21
10	3	0.50	0.15	0.65	0.13	0.09	0.23	0.09	0.02	0.11
	4	0.59	0.12	0.71	0.11	0.07	0.18	0.10	0.02	0.12
	5	0.48	0.09	0.57	0.15	0.09	0.24	0.18	0.02	0.19
	Mean	0.52	0.12	0.64	0.13	0.08	0.22	0.12	0.02	0.14
30	6	0.39	0.14	0.53	0.14	0.16	0.30	0.11	0.06	0.17
	7	0.37	0.12	0.48	0.15	0.20	0.35	0.08	0.09	0.17
	8	0.45	0.14	0.59	0.06	0.14	0.19	0.13	0.09	0.22
	Mean	0.40	0.13	0.53	0.11	0.17	0.28	0.10	0.08	0.19
80	9	0.33	0.09	0.42	0.08	0.37	0.45	0.03	0.10	0.13
	10	0.32	0.08	0.40	0.07	0.36	0.42	0.05	0.14	0.18
	11	0.31	0.08	0.39	0.02	0.24	0.26	0.09	0.27	0.36
	12	0.26	0.08	0.35	0.04	0.31	0.36	0.06	0.24	0.30
	Mean	0.31	0.08	0.39	0.05	0.32	0.37	0.06	0.19	0.24
120	13	0.21	0.12	0.33	0.04	0.35	0.39	0.02	0.59	0.61
	14	0.15	0.02	0.17	0.05	0.31	0.36	0.03	0.44	0.47
	15	0.16	0.05	0.21	0.05	0.25	0.30	0.03	0.46	0.49
	Mean	0.17	0.07	0.24	0.05	0.31	0.35	0.03	0.50	0.52

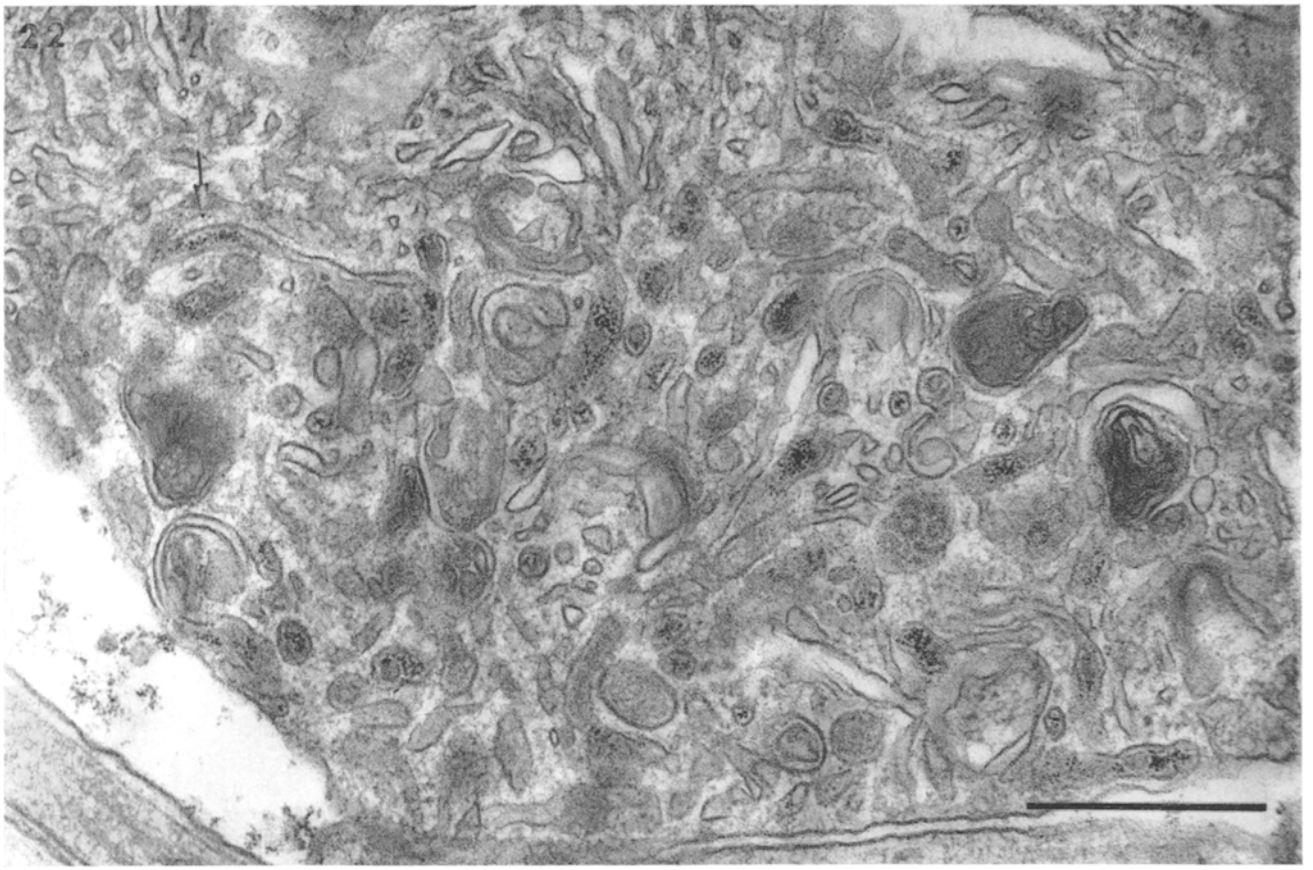
22

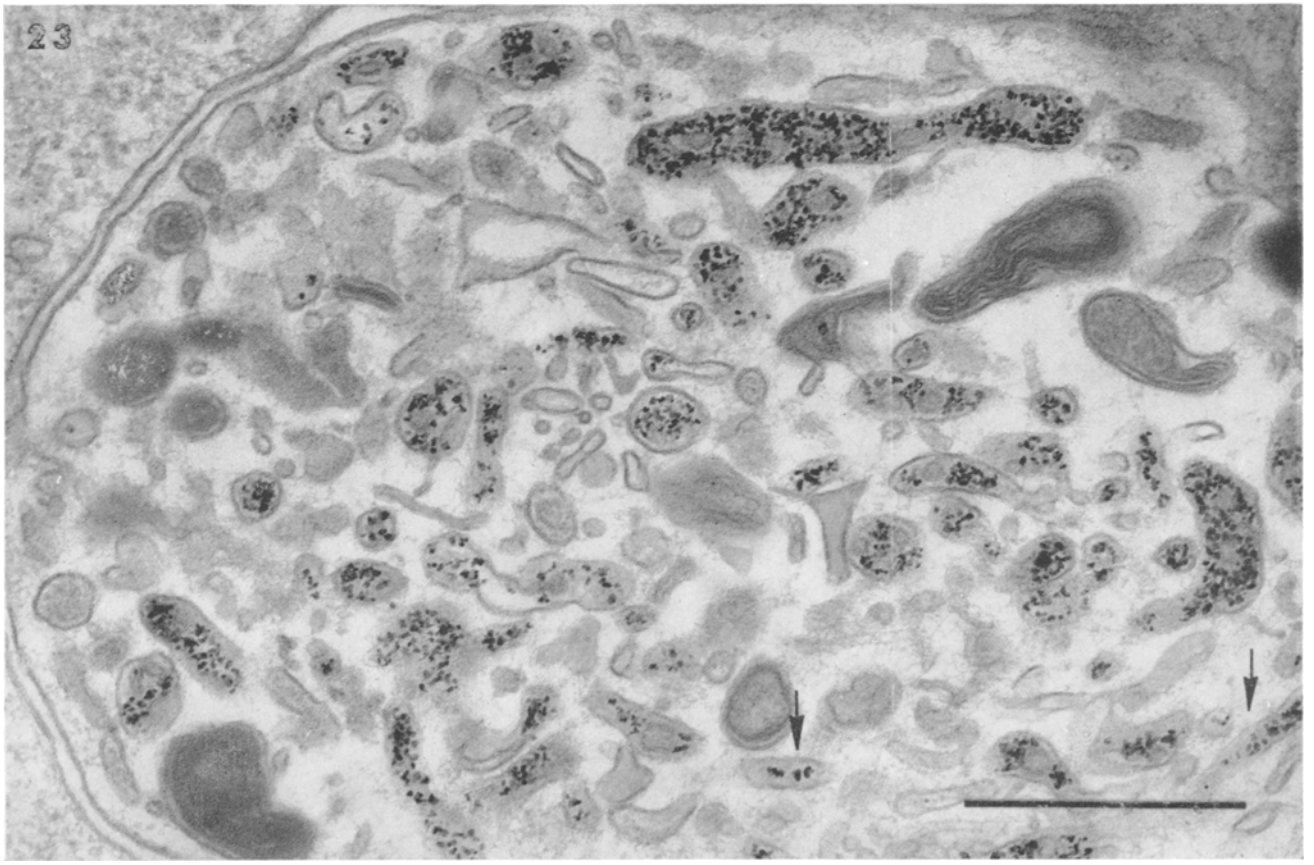
23

remained more or less constant. The labelled multi-vesicular body population (Fig. 34c) showed a similar rapid increase with time, but delayed with respect to the pre-multi-vesicular bodies. By 120 min over 90% of these organelles contained ferritin. The unlabelled population of multi-vesicular bodies declined somewhat more rapidly during the first 30 min than during the later exponential decline.

It is noteworthy that almost the entire population of pre-multi-vesicular bodies and multi-vesicular bodies took up ferritin within 2 h of exposure to the marker. Thus, if our assumption is correct that vacuoles form pre-multi-vesicular bodies and these in turn form multi-vesicular bodies, almost the entire population of unlabelled pre-multi-vesicular bodies and multi-vesicular bodies must have turned over in 2 h.

We would like now to examine whether or not this turnover is quantitatively consistent with this hypothesis. The model we propose is shown in Fig. 32, in which the unlabelled and labelled populations are treated independently. The treatment of the unlabelled elements was simplified by the fact that no assumptions had to be made about how the vacuoles were formed, they were simply taken as formed at $t = 0$. Values for the rate constants α, β and δ were determined through analysis of the following equations:

$$V(t + \triangle t) = (1 - \alpha \triangle t)\, V(t) \tag{1}$$

$$P(t + \triangle t) = (1 - \beta \triangle t)\, P(t) + \alpha \triangle t\, V(t) \tag{2}$$

$$M(t + \triangle t) = (1 - \delta \triangle t) M(t) + \beta \triangle t\, P(t) \tag{3}$$

In Equations 1 to 3, $V(t)$, $P(t)$, and $M(t)$ denote the fraction of the total unlabelled organelle population occupied by vacuoles, pre-multi-vesicular bodies, and multi-vesicular bodies respectively as functions of time (see Table 2). The constants α, β, and δ have the dimensions min^{-1} with respect to the relevant existing organelle population at each time under consideration. A least squares fit of the data of Table 2 based on Equations 1 to 3 gave $\alpha = 0.011\ \text{min}^{-1}$, $\beta = 0.046\ \text{min}^{-1}$, and $\delta = 0.068\ \text{min}^{-1}$. The solutions to Equations 1 to 3 with the above values for the rate constants are shown as solid lines in Fig. 34. In all cases the solutions were within the range of the observed values. We note also the existence of a broad predicted maximum in the $P(t)$ versus t curve at $t = 10$ min. The predicted V (t) and $M(t)$ functions are, on the other hand, decreasing monotonically over the period of the experiment.

In treating the labelled data within the context of the series model (Fig. 32) we had the additional difficulty of attempting to describe the time-course of pinocytosis of large vacuoles. If we denote the rate of labelled vacuole formation by $K^*(t)$, with the same dimensions as the other rate constants, and the populations of labelled organelles by $V^*(t)$, $P^*(t)$, and

---

Figs. 22 and 23 illustrate the extensive accumulation of labelled organelles in non-terminal varicosities from a 120 min ferritin experiment and a 120 min thorium experiment respectively. Most of the organelles containing marker are smooth-surfaced elements containing interior vesicles or dense cores; some of the label however is in simple tubules with no interior elements (arrows).

$M^{\star}(t)$, then the equations describing the time evolution of the labelled populations of organelles are:

$$V^{\star}(t + \triangle t) = (1 - \alpha^{\star} \triangle t)\, V^{\star}(t) + K^{\star}(t) \triangle t \quad (4)$$

$$P^{\star}(t + \triangle t) = (1 - \beta^{\star} \triangle t)\, P^{\star}(t) + \alpha^{\star} \triangle t\, V^{\star}(t) \quad (5)$$

$$M^{\star}(t + \triangle t) = (1 - \delta^{\star} \triangle t)\, M^{\star}(t) + \beta^{\star} \triangle t\, P^{\star}(t) \quad (6)$$

The rate constants, $\alpha^{\star}$, $\beta^{\star}$, $\delta^{\star}$, have the same meaning as in Equations 1 to 3. The best least squares fit of Equations 4 to 6 to the labelled data of Table 2, was obtained with $\alpha^{\star} = 0.073$ min^{-1}, $\beta^{\star} = 0.025$ min^{-1}, $\delta^{\star} = 0.025$ min^{-1}, and $K^{\star}(t)$ as shown in Fig. 33, where its value decreases approximately exponentially from a maximum at 10 min. Our data do not allow us to define the precise nature of the rising phase of $K^{\star}(t)$ during the interval 0 to 10 min. Attempts to fit the labelled data with two other forms of $K^{\star}(t)$, i.e. a single step function of 10 min duration, and a double step function of 30 min duration gave predicted labelling values quite inconsistent with the data. The calculated feeding function $K^{\star}(t)$ does in fact have the general form previously described for *Amoeba proteus* (Chapman–Andresen, 1962), although the time constant of decay is longer in our estimation. However, in HeLa cells pinocytosis may last for 5 h following a change of medium (Riedel and Gross, 1968).

The solutions of Equations 4 to 6 with the above values for $\alpha^{\star}$, $\beta^{\star}$, $\delta^{\star}$, and $K^{\star}(t)$, are shown as dashed lines in Fig. 34. For the most part the predicted variations of the labelled data with time fell within the range of the observations. The predicted 30 min pre-multi-vesicular body value is however, slightly greater than the observed values. A more serious discrepancy occurs at 120 min in the predicted versus actual multi-vesicular body values where the mean of the observations gives a fraction twice that calculated.

This analysis then indicates, particularly with regard to the unlabelled populations, that the postulate of transformation of pinocytotic vacuoles into multi-vesicular bodies via the pre-multi-vesicular bodies is quantitatively consistent with the observations. The analysis does, on the other hand, reveal difficulties with this simple scheme. The rate constant for

---

Figs. 24 to 30 from 120 min ferritin and thorium experiments show examples of the varieties of multi-vesicular bodies.

Fig. 24 shows a spherical form.

Fig. 25 shows a multi-vesicular body containing marker and continuous with a ring-shaped profile.

Fig. 26 shows a tubular multi-vesicular body with a cup-shaped terminal portion which contains marker.

Fig. 27 shows a labelled tubular multi-vesicular body from a 120 min thorium experiment.

Fig. 28 shows a multi-vesicular body with a distinctly tubular extension with no interior elements.

Fig. 29 shows apparent exocytosis of a multi-vesicular body: note the vesicles and thorium dioxide particles in the extracellular space.

Fig. 30 shows a labelled, elongated tubular multi-vesicular body from a 120 min ferritin experiment.

Fig. 31 shows two tubules with a regular diameter of 700 Å containing marker, a single interior vesicle and a dense core (arrows).

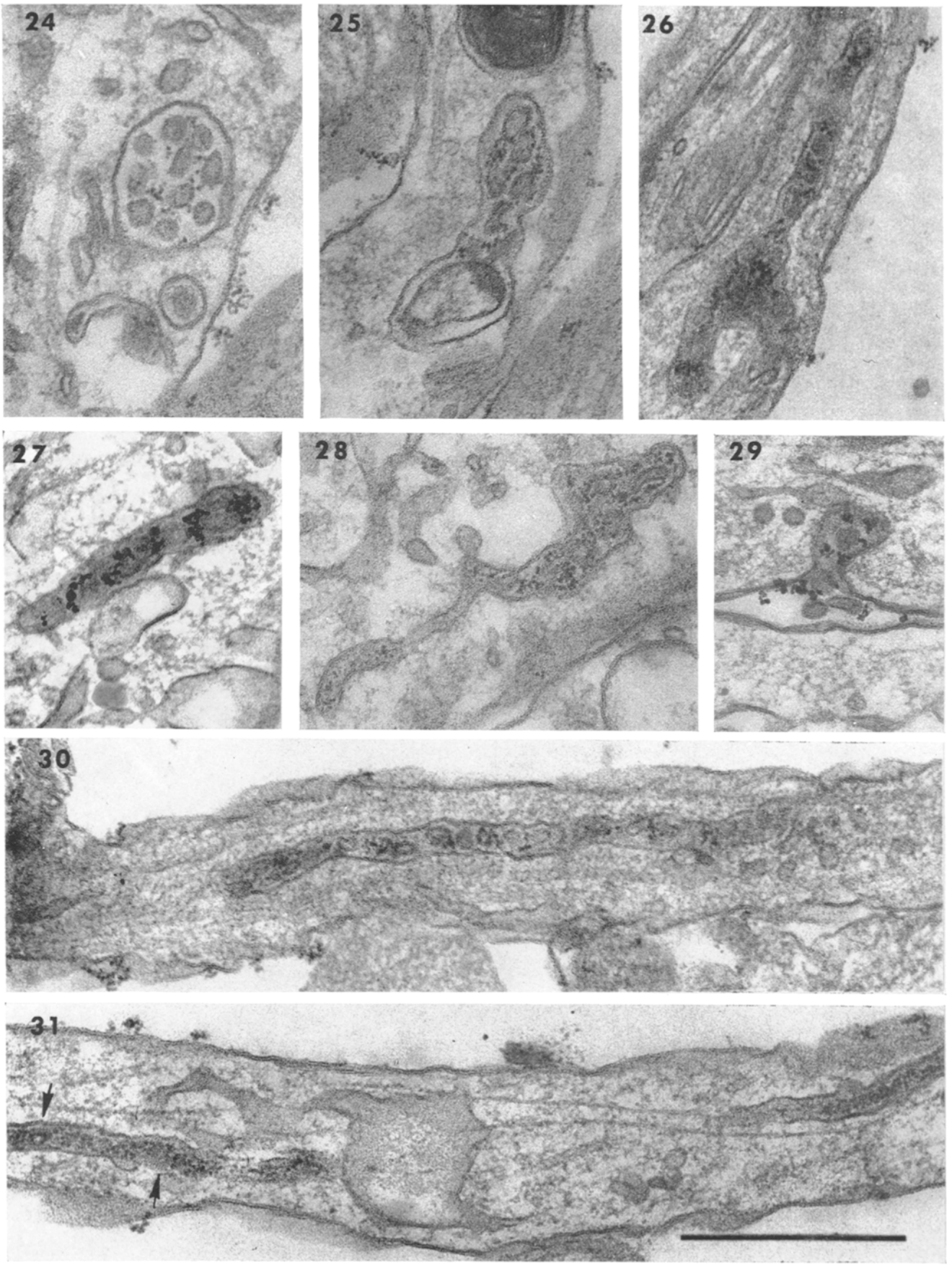
24
25
26
27
28
29
30
31

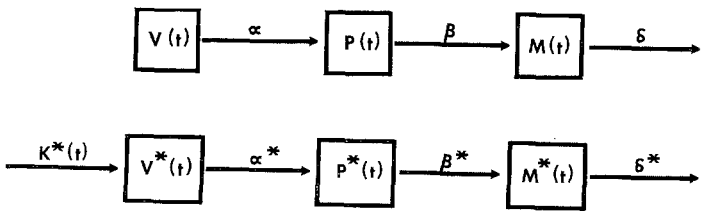

Fig. 32 Model for the formation of multi-vesicular bodies from pinocytotic vacuoles. The time dependent populations of vacuoles, pre-multi-vesicular bodies, and multi-vesicular bodies are denoted by $V(t)$, $P(t)$ and $M(t)$ respectively. The starred superscripts indicate a labelled quantity. The rate constants for transfer between populations are designated α, β, and δ, and for labelled vacuole formation $K^*(t)$.

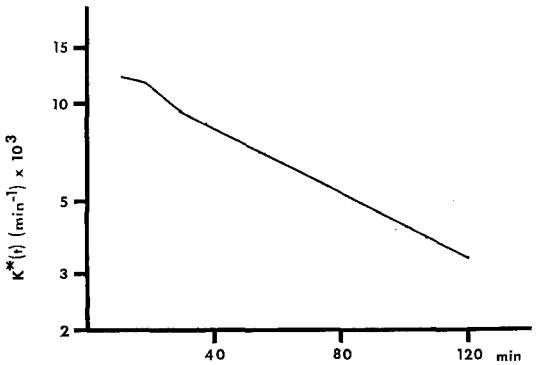

Fig. 33 The rate constant for labelled vacuole formation, $K^*(t)$, as a function of time. The values have the dimensions of min^{-1} with respect to the existing labelled vacuole population, and they were derived from a regression analysis of the labelled organelle data shown in Table 2 in conjunction with Equations 4 to 6 (see text).

transformation of labelled vacuoles to labelled pre-multi-vesicular bodies is nearly 7 times greater than for transformation of unlabelled vacuoles, whereas the other rate constants in the sequence of labelled populations are smaller than for the corresponding unlabelled ones. It would appear that the observed labelled vacuole population is too small to account for the subsequent transformations. The differences might be accounted for if in fact there was a second parallel input of label into the pre-multi-vesicular body population; but we have found no suggestion of other organelles fusing or combining with these organelles. It does not appear possible that either coated vesicles or dense-cored vesicles could transport label to the pre-multi-vesicular bodies. The coated and dense-cored vesicles usually contained 1 to 3 ferritin or thorium dioxide particles (Figs. 41–44, 46 and 47), whereas more than 20 particles were usually found in sections through pre-multi-vesicular bodies. Therefore, to account for the accumulation of particles in these organelles, many vesicles would have to have contributed their contents to them. If this were the case, the turnover rates for coated or dense-cored vesicles would be very high indeed, and our observations do not support this conclusion; even following a 2 h incubation, as noted earlier, only 50% of the coated vesicles

and 4% of the dense-cored vesicles were labelled, and in each case the labelled populations represented less than 5% of the total number of labelled organelles in the tissue.

An alternative explanation is that the counting of labelled and unlabelled vacuoles was in error. Because of the high concentration of label in the pre-multi-vesicular bodies and in multi-vesicular bodies, it was a simple matter in surveying the tissues in the electron microscope to differentiate between labelled and unlabelled individuals. The low concentration of label in the vacuoles (sometimes only one particle was present cf. Figs. 11 and 12), introduced uncertainty in distinguishing which vacuoles were in fact labelled when scanning the sections. If label was not present in sections through some of the labelled vacuoles, then we would have erred further in our counting, with the result that the numbers of labelled vacuoles would have been underestimated and unlabelled ones overestimated. Furthermore, some fraction of the unlabelled vacuoles may not be of pinocytotic origin (Tennyson, 1970). Correction of these errors would reduce the unlabelled and increase the labelled vacuole population, and reduce the rate constant (α^*) for transfer of label from vacuoles to pre-multi-vesicular bodies and increase the rate constant (α) for the unlabelled populations to bring them closer together. By suitable adjustment of $K^*(t)$, describing the formation of labelled vacuoles, the behaviour of the labelled and unlabelled populations could then be made to coincide more closely. We have not made these calculations because of uncertainties in determining the counting error and in defining $K^*(t)$ with assurance. We feel, therefore, as noted above, that the one conclusion to be drawn from this analysis is that the numerical data are quantitatively consistent with the proposed series pathway.

The pile-up of labelled multi-vesicular bodies following 2 h incubation with ferritin (Fig. 34c) is anomalous, and apparently long lasting for, as described below, in one experiment with thorium dioxide there were still large numbers of labelled multi-vesicular bodies in the tissue 16 h following a 2 h incubation with label. It may reflect a saturation of the transfer mechanisms, perhaps related to the acquisition of lysosomal hydrolases from the soma (Novikoff, 1967, and discussion below). On the other hand, the high concentration of markers in the multi-vesicular bodies may interfere with movement through the pathway. In view of this possibility, and the fact that no assumptions about the formation of unlabelled vacuoles were necessary in our calculations, more reliance probably should be placed on the analysis of the unlabelled populations than on the labelled ones.

Experiments with aged ferritin and with thorium dioxide

We have not followed successfully the fate of labelled multi-vesicular bodies in detail, for a number of reasons that will be apparent in what follows. As noted above, after 120 min incubation with ferritin there was distinct, although limited, labelling of blind-ended tubules which bore striking similarities to the regular diameter multi-vesicular bodies. The significance of labelling of these structures was emphasized in one experiment in which ganglia were incubated for 120 min with a preparation of ferritin that had been stored for several years in the cold. In the ganglia incubated with this ferritin there was a heavy uptake of marker by vacuoles, pre-multi-vesicular bodies and multi-vesicular bodies. Of particular interest, however, was the fact that large numbers of blind-ended tubules with a regular diameter of 700 Å, varying in length from 0.4 μm to over 3 μm contained large amounts of

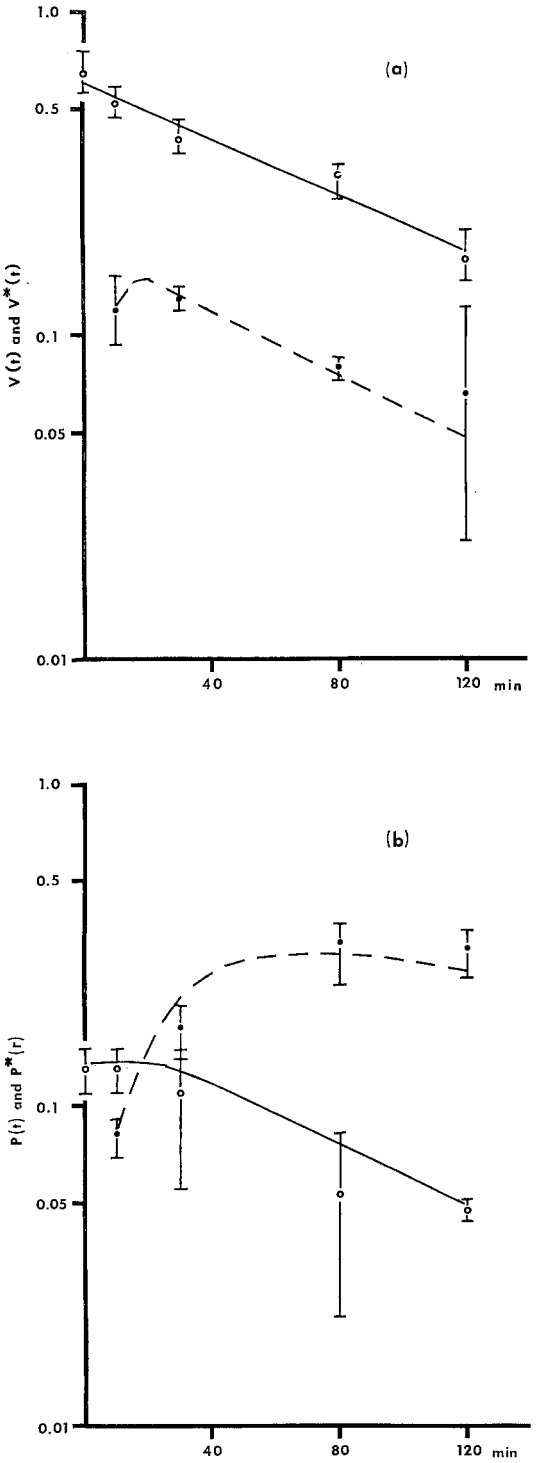
(a)
1.0
0.5
0.1
0.05
0.01
V(t) and V*(t)
40
80
120 min
(b)
1.0
0.5
0.1
0.05
0.01
P(t) and P*(t)
40
80
120 min

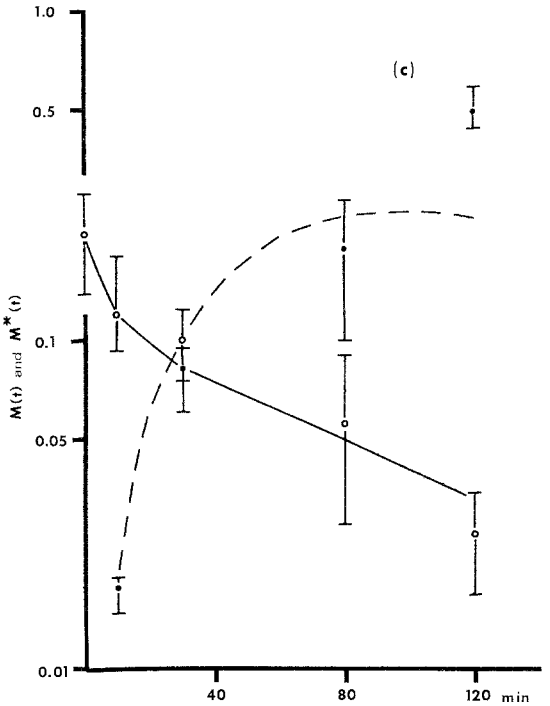

Fig. 34. Variations in unlabelled and labelled organelle populations, expressed as a fraction of the total population of vacuoles, pre-multi-vesicular bodies and multi-vesicular bodies, with time after administration of ferritin. The means of the observed values are shown by circles (open circles for unlabelled) and the range of the observed values by vertical bars. The solid and dashed lines are the solutions of Equations 1 to 3, and 4 to 6 (see text) for unlabelled and labelled populations respectively and the symbols have the same meaning as in Fig. 32. (a) shows the variation in vacuole population, (b) in pre-multi-vesicular body population and (c) in multi-vesicular body population.

ferritin (Fig. 35). These tubules were often aligned end-to-end along the neurites (Fig. 36) and constrictions suggestive of pinching off or fusion were found (Fig. 37). Some of these elements contained vesicles or discrete dense cores in their interiors (Fig. 38). On the series hypothesis we have proposed, these observations support the suggestion, derived from the earlier group of experiments, that blind-ended tubules can form from tubular multi-vesicular bodies.

Of equal significance was that, despite the extensive labelling of blind-ended tubules, there was little labelling of the endoplasmic reticulum. Furthermore, in this same experiment three ganglia were, after the incubation, washed free of ferritin and incubated an additional 120 min before fixation. Again, little labelling of the endoplasmic reticulum was found. Where ferritin was found in this system, it was only as scattered isolated particles, and our identification was therefore somewhat uncertain.

To overcome this problem we did a number of further experiments with the more electron-dense marker thorium dioxide and extended the chase periods to 16 h. With a 120 min incubation with thorium the intracellular distribution of labelled organelles was certainly

qualitatively similar to that found with ferritin (Fig. 23), and thorium was readily identifiable in the endoplasmic reticulum (Fig. 39); however the incidence of labelling of this system was low. Even with a 16 h chase period there was no dramatic shift in the distribution of label into the endoplasmic reticulum. Most of the labelled organelles were multivesicular bodies and only a small fraction of the vacuoles and pre-multi-vesicular bodies were labelled.

These observations with thorium and aged ferritin then support the sub-division of the intracellular tubular systems into two parts, the endoplasmic reticulum and the blind-ended tubular system, a division made above on purely morphological grounds. In addition, they suggest that within the time period of these experiments the blind-ended tubular system is not an intermediate in the formation of endoplasmic reticulum from primary pinocytotic elements.

The thorium experiments also permitted a more precise identification of labelled dense-cored vesicles because of the high density of the marker. After a 120 min incubation labelled dense-cored vesicles were readily identified; however, as with the experiments with ferritin, only 3–4% were labelled at this time, and they again only comprised 2% of the total labelled organelles. About 60% of these labelled organelles were from 1000–1300 Å in diameter with a fairly homogeneous, coarsely granular core of light-to-moderate electron density (Fig. 41). This population is similar to that described by Lentz (1967) in regenerating amphibian nerve and thought to be of perikaryal origin. The core filled most of the interior of the vesicles and was usually separated from the vesicle membrane by a narrow electron lucent band. Profiles resembling membrane fragments were occasionally seen in the core region (Fig. 40). Thorium was also located in a group of smaller dense-cored vesicles (Figs. 42 and 44), averaging 850 Å in diameter, and with more compact and electron-dense cores. This group is similar to the dense-cored vesicles found in the proximal stumps of interrupted mature peripheral nerve (cf. Pellegrino de Iraldi and de Robertis, 1968; Geffen and Ostberg, 1969). In these vesicles, the core was finely granular with a diameter of 450 Å and was occasionally surrounded by a unit membrane, distinct from the limiting membrane of the vesicle (Fig. 43). Dense-cored vesicles of this same character were observed frequently with small curved or straight tails (Figs. 20 and 21), and short blind-ended tubules with discrete dense cores or with overall dense matrices (Figs. 40, 43, 44 and 45), also contained marker. Similar structures to these have been reported previously in this tissue (Holtzman, 1971)

Figs. 35 to 38 from a 120 min 'aged' ferritin experiment showing extensive accumulation of ferritin in regular diameter tubules in the neurites.

Fig. 35. The elongated tubule is not seen to be blind-ended.

Fig. 36. At least three blind-ended tubules are aligned end to end along the neurite, and the walls of one of these (arrow) are dilated.

Fig. 37 shows a tubule with a constricted region (arrow) suggestive of fusion or pinching off.

Fig. 38. The tubule contains a single interior vesicle (arrow).

Fig. 39 from a 120 min thorium experiment shows the presence of marker in elements of the endoplasmic reticulum (arrows) in a non-terminal varicosity.

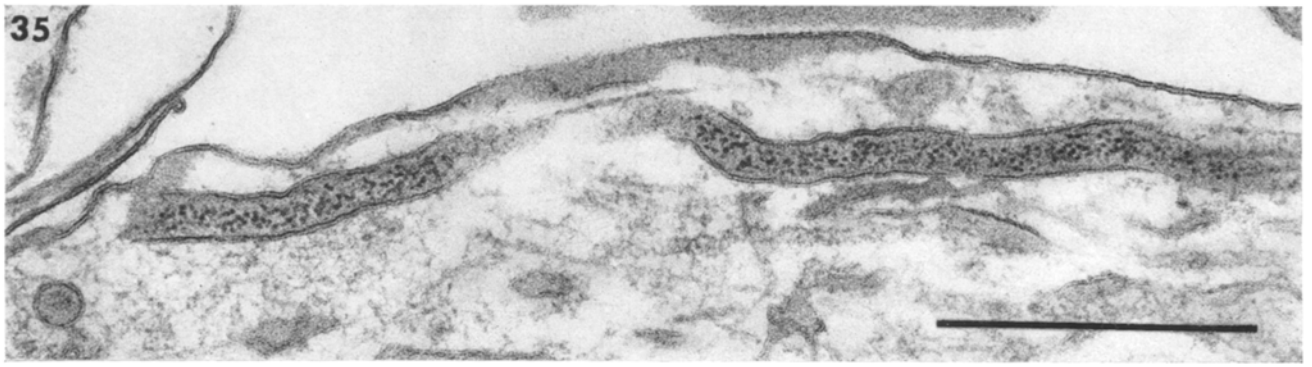
35


36

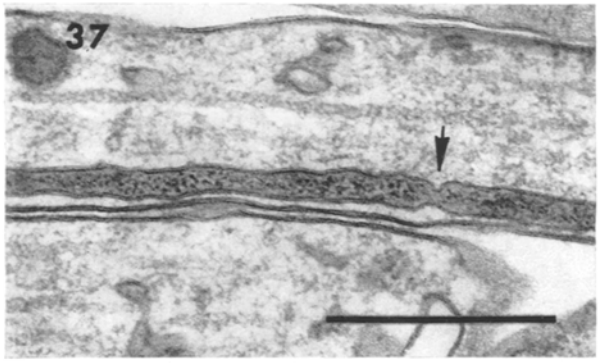
37

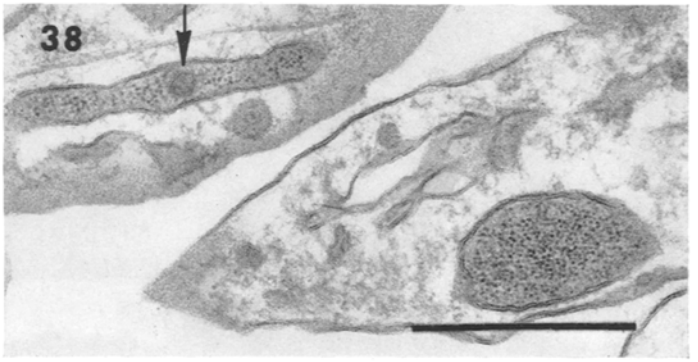
38

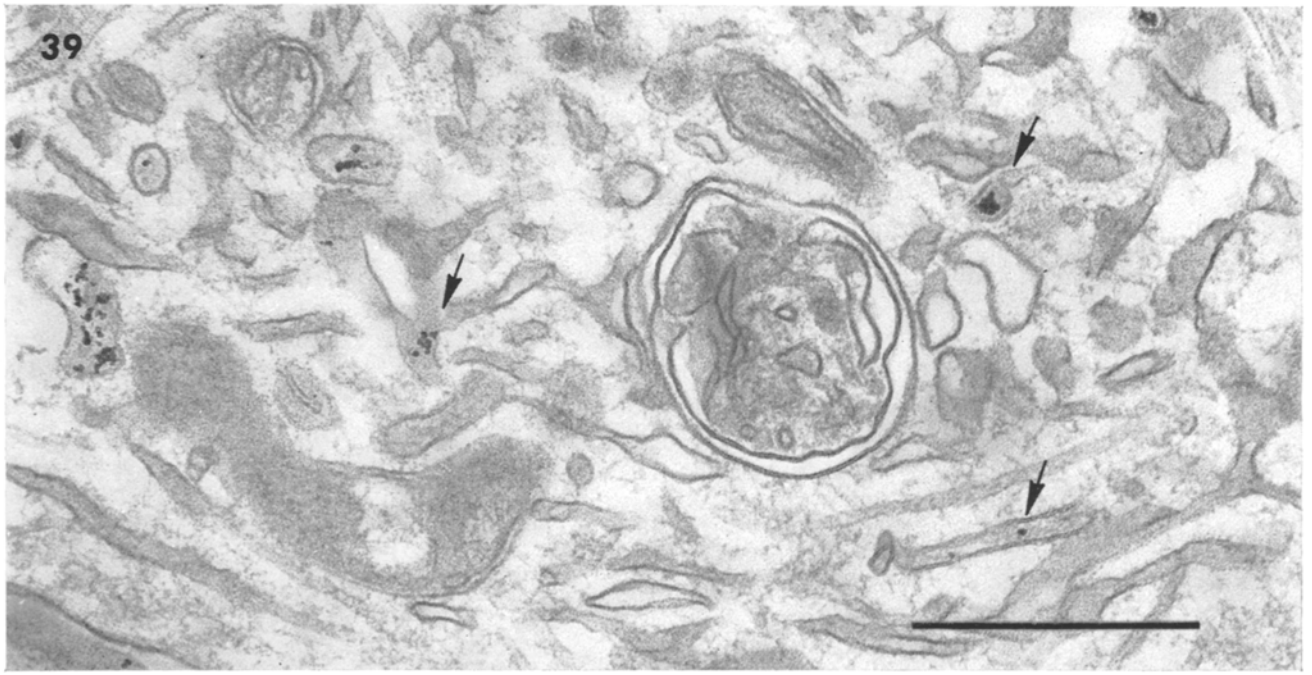
39

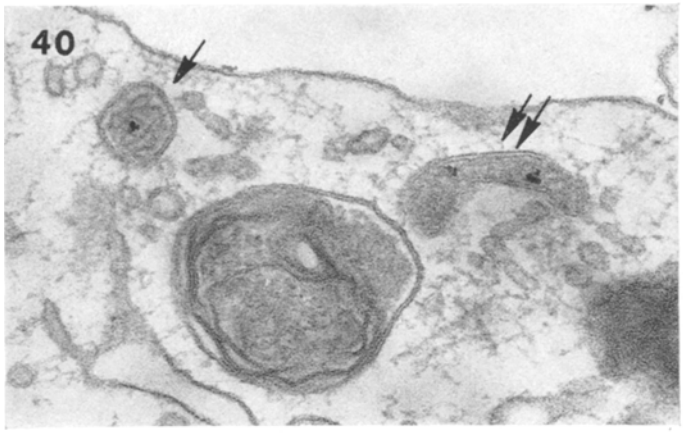
40

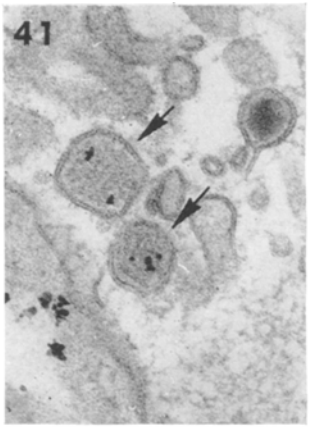
41

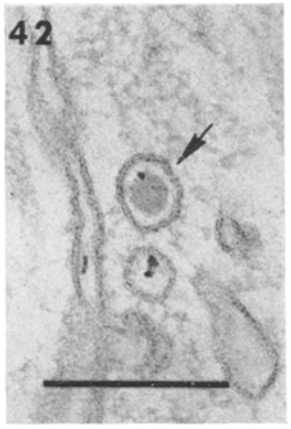
42

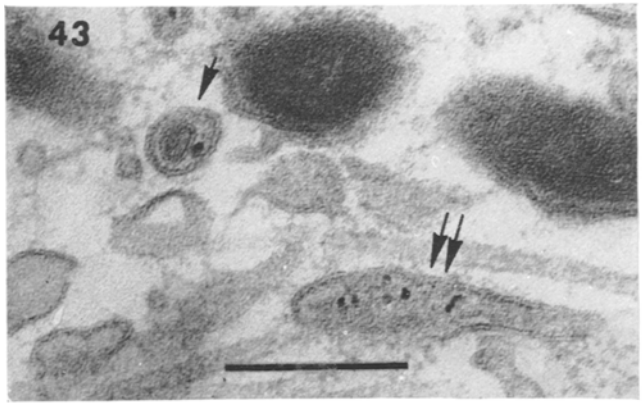
43

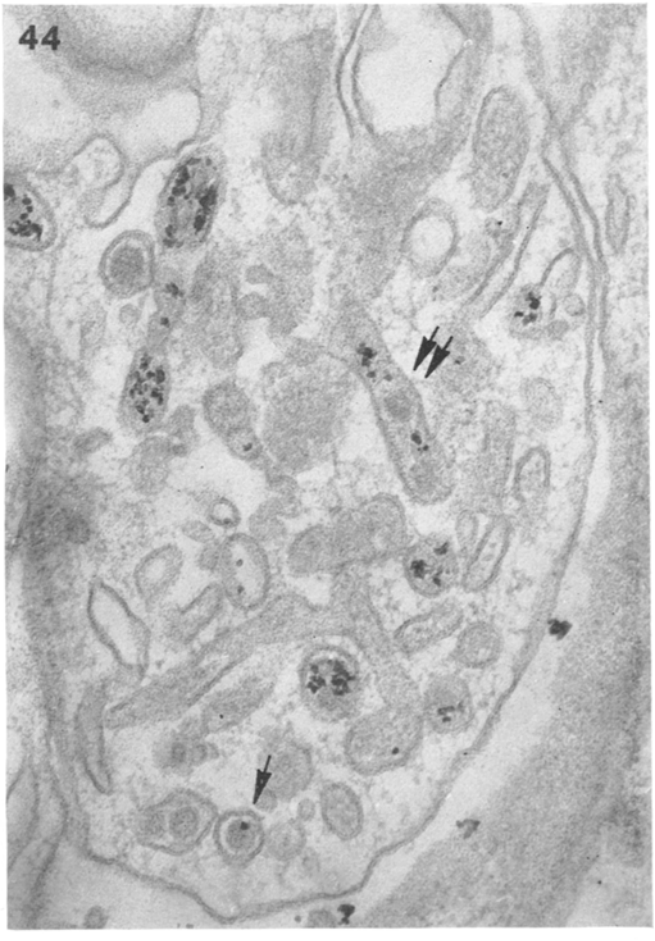
44

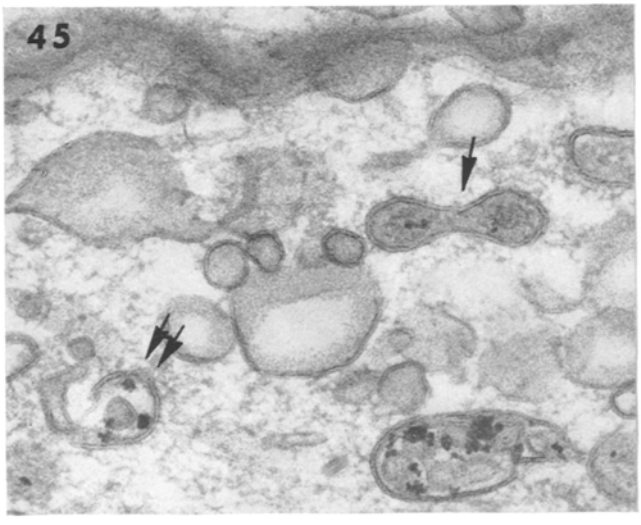
45

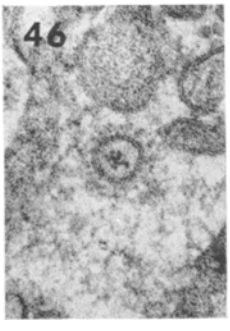
46

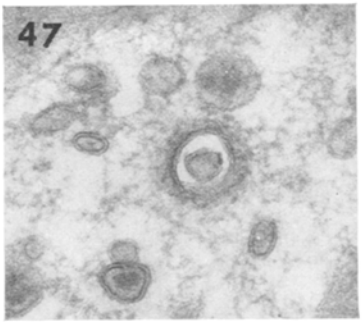
47


48

and in mature interrupted nerve (Pellegrino de Iraldi and de Robertis, 1968) and were thought to form part of the endoplasmic reticulum and to give rise to dense-cored vesicles.

Uptake of markers into coated vesicles (Fig. 46), a few of which contained an interior vesicle or dense core (Fig. 47) was also observed, and we have obtained clear evidence of formation of these organelles by pinocytosis (Fig. 48), as is known for other tissues. It must be pointed out, however, that the number of coated vesicles, labelled and unlabelled, was small (about 3% of the total labelled organelles again) compared to the numbers of labelled and unlabelled vacuoles, pre-multi-vesicular bodies and multi-vesicular bodies. This emphasizes, as we have noted earlier, that uptake of extracellular material by coated vesicles, or for that matter, by dense-cored vesicles, is small in this tissue compared with the pathway we have outlined (cf. Rosenbluth and Wissig, 1964; Zacks and Saito, 1969).

In these thorium experiments we also observed instances of possible exocytosis of labelled spherical multi-vesicular bodies (Fig. 29), but the number was small.

Uptake of ferritin by decentralized neurites

We have followed the uptake of ferritin into neurites severed from their cell bodies. Using a razor blade, cuts were made through the neuritic halo around the periphery of the mass of somas; the cell bodies were then removed and discarded without disturbing the neuritic outgrowth. The isolated neurites were then incubated with ferritin or thorium dioxide for 2 h and fixed and embedded in the usual way.

No obvious morphological alterations were observed in the decentralized neurites and the uptake and intracellular distributions of the tracers did not appear to differ from intact preparations incubated with the marker for similar periods. These findings are in accord with the observation (Hughes, 1953) that cultured neurites severed from their cell bodies continue normal growth for up to 3 h.

Figs. 40 to 48 illustrate the varieties of dense-cored and coated vesicles that accumulate marker following 120 min incubation with thorium or ferritin.

Fig. 40. The dense core (single arrow) of the large labelled vesicle exhibits a substructure suggestive of membrane fragments. Marker is also present in a tubule containing dense material (double arrows).

Fig. 41. Marker is present in two large vesicles with moderately dense cores which fill most of the interiors (single arrows).

Figs. 42, 43 and 44 show marker in smaller dense-cored vesicles with compact cores (single arrows) and in one of these (Fig. 43) the core is delimited by a clearly defined unit membrane. Marker is also present in tubules containing uniformly distributed dense material (Fig. 43) or discrete dense cores (Fig. 44) (double arrows).

Fig. 45 shows labelling of a dumbell-shaped structure containing two dense cores (single arrow). Marker is also present in two small multivesicular bodies, one of which (double arrows) contains only one interior vesicle.

Figs. 46 and 47 demonstrate the presence of marker within coated vesicles. A coated vesicle containing a single interior vesicle is shown in Fig. 47.

Fig. 48 shows a coated invagination of the neuritic plasmalemma. The bar in this figure represents 0.5 μm for Figs. 40, 41, 44–8. The bars in Figs. 42 and 43 represent 0.2 μm.

Discussion

Our experiments have shown that a variety of intracellular organelles in growing axons take up extracellular tracers in a fashion which suggests that they are formed locally from the plasma membrane during pinocytosis. Our results are quantitatively consistent with the hypothesis that primary pinocytotic vacuoles are the precursors of pre-multi-vesicular bodies and these in turn form multi-vesicular bodies. Suggestions along this line have been made by earlier workers; thus Novikoff (1967) has proposed that multi-vesicular bodies are formed from pinocytotic vacuoles through interaction with primary lysosomes in mature nervous tissue, and Holtzman and co-workers in studies on the adrenal medulla and on cultured sensory ganglia have proposed that cup-shaped vacuoles may be precursors of multi-vesicular bodies (Holtzman and Dominitz, 1968; Holtzman and Peterson, 1969). Our observations also provide suggestive evidence that tubular multi-vesicular bodies are converted into blind-ended tubules of regular diameter; but within the time span of our experiments we have not obtained evidence that the blind-ended tubules are precursors of endoplasmic reticulum. Only scattered bits of marker are found in the endoplasmic reticulum even after prolonged incubation, suggesting that this system only rarely connects with blind-ended tubules or with extracellular space. This also seems to be the case at adult frog motor nerve endings (Birks, 1966).

Perhaps it is reasonable to view the labelling of dense-cored vesicles, particularly the smaller 850 Å diameter class, as arising by a related process to that which is involved in the formation of multi-vesicular bodies. Such a process originating in pinocytosis of small vacuoles or vesicles would satisfactorily account for the observation that the inner cores were quite often found to be surrounded by a limiting membrane. Thus dense-cored vesicles of this class may form from pinocytotic vesicles via intermediates in which a single interior vesicle forms. Certainly the sizes of the interior vesicles and cores was about the same as those found in the pre-multi-vesicular bodies and the multi-vesicular bodies. The large dense-cored vesicles do not fit this scheme, for they contained larger and less-dense cores than did the smaller group or the multi-vesicular bodies, and they were never seen with an inner vesicle outline. Coated vesicles sometimes contained either large of small dense cores. There is evidence that coated vesicles can lose their external coats (Gray and Willis, 1970), thus coated vesicles might provide an alternate peripheral pathway for formation of dense-cored vesicles.

If the line of reasoning we have developed is substantially correct then we may draw the conclusion that many of the tubular and vesicular organelles at growing neurites derive their limiting membranes from plasmalemma ingested in the process of pinocytosis. We have obtained some indications as to how these transformations take place. The concentration of ferritin in the cup-shaped vacuoles suggests that they form from collapse of spherical vacuoles. In addition the existence of various intermediate forms suggests that tubular multi-vesicular bodies form from elongation of cup-shaped vacuoles. It is interesting that a sphere 0.4 μm in diameter has the same surface area as a tube 700 Å diameter and 2.3 μm long; these are about the upper limits for the dimensions of the spherical vacuoles and blind-ended

tubules we have seen. The amount of plasmalemma incorporated into a typical spherical vacuole would therefore be sufficient to form a blind-ended tubule.

The presence of internal vesicles and dense cores within the transforming elements may, however, indicate that a more active process is involved. We have occasionally observed invaginations of the surface of multi-vesicular bodies suggesting that some interior vesicles form by a process analagous to pinocytosis (cf. Hirsch, Fedorko and Cohn, 1968). However, frequently the matrix of the inner vesicles exhibited high electron density. Similar vesicles, staining intensely with OsO_4, have been reported in multi-vesicular bodies of rat epididymis and on the basis of cytochemical studies were suggested to originate in the Golgi apparatus (Friend, 1969). To account for the widely reported presence of lysosomal enzyme activities in multi-vesicular bodies, it has also been suggested that the inner vesicles represent primary lysosomes transported from the Golgi apparatus into the multi-vesicular bodies (Novikoff, 1967). If we may use this information from other tissues, it would appear that other subcellular organelles may be involved in the formation of multi-vesicular bodies, with the plasmalemma providing the source of limiting membrane.

Finally, our findings may be of some relevance in interpreting the results of nerve ligation studies. When mature peripheral nerves are interrupted either by ligation, section, or compression there is a marked increase in the organelle population of the axons proximal to the interruption (for references see Martinez and Friede, 1970). The origin of these organelles is usually considered to be the cell bodies of the affected axons, and the accumulation to result from a variety of forms of peripherally directed axoplasmic transport. As we have noted throughout the text, these organelle accumulations are clearly similar to those described here in the varicosities of the growing neurites. This is particularly true with respect to the electron lucent and dense-cored tubule and vesicle populations which we have shown to have, to a considerable extent, a peripheral origin in the growing neurites. Zelená *et al.* (1968) have shown that local active nerve regeneration begins as early as 4 h after interruption; thus the organelle accumulation at interrupted axons may result partly from a local uptake of plasma membrane during recovery from injury, not solely from a somatofugal migration of organelles.

Acknowledgements

We would like to express our thanks to Mr William Mullin for generous assistance with some of these experiments and to the Medical Research Council of Canada for financial support.

References

BIRKS, R. I. (1966) The fine structure of motor nerve endings at frog myoneural junctions. *Annals of the New York Academy of Sciences* **135**, 8–19.

BIRKS, R. I. and WELDON, P. R. (1971) Formation of crystalline ribosomal arrays in cultured chick embryo dorsal root ganglia. *Journal of Anatomy (London)* **109**, 143–56.

CHAPMAN-ANDRESEN, C. (1962) Studies on pinocytosis in Amoebae. *Comptes Rendus des Travaux du Laboratoire Carlsberg* **33**, 73–264.

FRIEND, D. S. (1969) Cytochemical staining of multivesicular body and Golgi vesicles. *Journal of Cell Biology* **41**, 269–79.

GEFFEN, L. B. and OSTBERG, A. (1969) Distribution of granular vesicles in normal and constricted sympathetic neurones. *Journal of Physiology (London)* **204**, 583–92.

GRAY, E. G. and WILLIS, R. A. (1970) On synaptic vesicles, complex vesicles and dense projections. *Brain Research* **24**, 149–68.

HIRSCH, J. G., FEDORKO, M. E. and COHN, Z. A. (1968) Vesicle fusion and formation at the surface of pinocytotic vacuoles in macrophages. *Journal of Cell Biology* **38**, 629–32.

HOLTZMAN, E. (1971) Cytochemical studies of protein transport in the nervous system. *Philosophical Transactions of The Royal Society of London Series B* **261**, 407–21.

HOLTZMAN, E. and DOMINITZ, R. (1968) Cytochemical studies of lysosomes, Golgi apparatus and endoplasmic reticulum in secretion and protein uptake by adrenal medulla cells in the rat. *Journal of Histochemistry and Cytochemistry* **16**, 320–36.

HOLTZMAN, E. and PETERSON, E. R. (1969) Uptake of protein by mammalian neurones. *Journal of Cell Biology* **40**, 863–9.

HUGHES, A. (1953) The growth of embryonic neurites. A study on cultures of chick neural tissues. *Journal of Anatomy* (London) **87**, 150–62.

KAPELLER, K. and MAYOR, D. (1969) An electron microscopic study of the early changes proximal to a constriction in sympathetic nerves. *Proceedings of the Royal Society of London Series B*, **172**, 39–51.

KAWANA, E., SANDRI, C. and AKERT, K. (1971) The ultrastructure of growth cones in the cerebellar cortex of the neonatal rat and cat. *Zeitshrift für Zellforschung und mikroskopische Anatomie* **115**, 284–98.

LENTZ, T. L. (1967) Fine structure of nerves in the regenerating limb of the newt Triturus. *American Journal of Anatomy* **121**, 647–70.

MARTINEZ, A. J. and FRIEDE, R. L. (1970) Accumulation of axoplasmic organelles in swollen nerve fibres. *Brain Research* **19**, 183–98.

NOVIKOFF, A. B. (1967) Lysosomes in nerve cells. In *The Neuron*. (ed. H. HYDÉN) pp. 319–77. New York: Elsevier.

PELLEGRINO DE IRALDI, A. and DE ROBERTIS, E. (1968) The neurotubular system of the axon and the origin of granulated and non-granulated vesicles in regenerating nerves. *Zeitshrift für Zellforschung und mikroskopische Anatomie* **87**, 330–44.

POMERAT, C. M., HENDELMAN, W. J., RAIBORN, C. W. and MASSEY, J. M. (1967) Dynamic activities of nervous tissue *in vitro*. In *The Neuron* (ed. H. HYDÉN) pp. 119–78. New York: Elsevier.

RIEDEL, B. and GROSS, W. O. (1968) Mikropinocytose während der stillen Periode der diskontinuierlichen Pinocytose in der Gewebekultur. *Zeitshrift für Zellforschung und mikroskopische Anatomie* **92**, 360–6.

ROBBINS, E. and GONATAS, N. K. (1964) *In vitro* selection of the mitotic cell for subsequent electron microscopy. *Journal of Cell Biology* **20**, 356–9.

ROSE, G. G., POMERAT, C. M., SHINDLER, T. O. and TRUNNELL, J. B. (1958) A cellophane strip technique for culturing tissue in multipurpose culture chambers. *Journal of Biophysical and Biochemical Cytology* **4**, 761–4.

ROSENBLUTH, J. and WISSIG, S. L. (1964) The distribution of exogenous ferritin in toad spinal ganglia and the mechanism of its uptake by neurones. *Journal of Cell Biology* **23**, 307–25.

TENNYSON, V. M. (1970) The fine structure of the axon and growth cone of the dorsal root neuroblast of the rabbit embryo. *Journal of Cell Biology* **44**, 62–79.

YAMADA, K. M., SPOONER, B. S. and WESSELLS, N. K. (1971) Ultrastructure and function of growth cones and axons of cultured nerve cells. *Journal of Cell Biology* **49**, 614–35.

ZACKS, S. I. and SAITO, A. (1969) Uptake of exogenous horseradish peroxidase by coated vesicles in mouse neuromuscular junctions. *Journal of Histochemistry and Cytochemistry* **17**, 161–70.

ZELENÁ, J., LUBINSKA, L. and GUTMANN, E. (1968) Accumulation of organelles at the ends of interrupted axons. *Zeitschrift für Zellforschung und mikroskopische Anatomie* **91**, 200–19.